OAK RIDGE NATIONAL LABORATORY LIBRARIES
3 4456 0548400 8

CENTRAL RESEARCH LIBRARY
DOCUMENT COLLECTION

OAK RIDGE NATIONAL LABORATORY
operated by
UNION CARBIDE CORPORATION
NUCLEAR DIVISION
for the
U.S. ATOMIC ENERGY COMMISSION

UNION CARBIDE

ORNL-TM-1312
Volume 8

44

STRUCTURAL ANALYSIS OF SHIPPING CASKS
VOL. 8. EXPERIMENTAL STUDY OF THE STRESS-STRAIN PROPERTIES OF LEAD UNDER SPECIFIED IMPACT CONDITIONS

(Thesis)

J. H. Evans

OAK RIDGE NATIONAL LABORATORY
CENTRAL RESEARCH LIBRARY
DOCUMENT COLLECTION
LIBRARY LOAN COPY
DO NOT TRANSFER TO ANOTHER PERSON
If you wish someone else to see this document, send in name with document and the library will arrange a loan.
UCN-7969
(3 3-67)

Submitted as a thesis to the Graduate Council of the University of Tennessee in Partial fulfillment of the requirements for the Master of Science Degree.

LEGAL NOTICE

This report was prepared as an account of Government sponsored work. Neither the United States, nor the Commission, nor any person acting on behalf of the Commission:

A. Makes any warranty or representation, expressed or implied, with respect to the accuracy, completeness, or usefulness of the information contained in this report, or that the use of any information, apparatus, method, or process disclosed in this report may not infringe privately owned rights; or

B. Assumes any liabilities with respect to the use of, or for damages resulting from the use of any information, apparatus, method, or process disclosed in this report.

As used in the above, "person acting on behalf of the Commission" includes any employee or contractor of the Commission, or employee of such contractor, to the extent that such employee or contractor of the Commission, or employee of such contractor prepares, disseminates, or provides access to, any information pursuant to his employment or contract with the Commission, or his employment with such contractor.

ORNL TM-1312
Vol. 8

Contract No. W-7405-eng-26

General Engineering Division

STRUCTURAL ANALYSIS OF SHIPPING CASKS
VOL. 8. EXPERIMENTAL STUDY OF THE STRESS-STRAIN PROPERTIES OF LEAD UNDER SPECIFIED IMPACT CONDITIONS

J. H. Evans

The material contained herein was submitted to the Graduate Council of the University of Tennessee in partial fulfillment of the requirements for the Master of Science Degree with a major in Mechanical Engineering

AUGUST 1970

OAK RIDGE NATIONAL LABORATORY
Oak Ridge, Tennessee
operated by
UNION CARBIDE CORPORATION
for the
U.S. ATOMIC ENERGY COMMISSION

OAK RIDGE NATIONAL LABORATORY LIBRARIES
3 4456 0548400 8

ACKNOWLEDGMENTS

The author wishes to express his gratitude to Dr. Frank H. Speckhart of the Mechanical Engineering Department of The University of Tennessee for his advice and time spent reviewing the material in this document. The author also wishes to express his appreciation to Messrs. B. C. Duggins and C. B. Williams of the Instrumentation and Controls Division at Oak Ridge National Laboratory for their assistance with the instrumentation for this project and to Mr. W. C. Stoddart of the General Engineering Division at Oak Ridge National Laboratory for his assistance in writing the computer program.

ABSTRACT

The purpose of this investigation was to determine the stress-strain properties of lead subjected to gross compressive strains at strain rates comparable to those experienced by lead shielding in shipping containers for radioactive materials under accident conditions. A survey of technical literature related to the experimental determination of dynamic stress-strain relationships for metals revealed a general lack of documentation of the materials tested and that the strain rates used in these investigations were not generally in the range desired for the purpose of this investigation. The needed data were therefore developed in an experimental test program.

Right circular cylinders of chemical lead with five different geometries were impacted by free-falling steel cylinders of three different weights dropped from various heights. The force was measured and recorded as a function of time by using a resistance-strain-gage load cell, amplifier, oscilloscope, and a Polaroid camera. A computer program was written to numerically integrate the force-with-respect-to-time data to obtain velocity-with-respect-to-time and displacement-with-respect-to-time data. From these data, a stress-strain curve was plotted and an approximate equation for this curve was written.

It was found that the empirical equation described the dynamic true stress-strain curve for chemical lead and that the curve for this equation demonstrated reasonable agreement with the experimental data at strains up to 0.5 inch per inch. It was concluded that the dynamic stress-strain relationship for chemical lead expressed by this equation

can be applied in actual design problems with approximately the same accuracy as is normally encountered when published material property data are used.

TABLE OF CONTENTS

SECTION	PAGE
1. INTRODUCTION	1
Demonstrating Compliance With the Regulations	2
Determination of Stress-Strain Properties of Lead Under Impact Conditions	4
2. REVIEW OF LITERATURE	5
3. DEVELOPMENT OF TEST PROGRAM AND APPARATUS	14
Test Philosophy	14
Design of Test Facility and Instrumentation	15
Instrument Calibration and Preliminary Test	17
Selection of Test Material and Fabrication of Specimens	22
4. PERFORMANCE OF IMPACT TESTS	25
5. DATA TRANSFORMATION AND EVALUATION	31
The Computer Program	31
Evaluation of Computer Output	41
6. SUMMARY, CONCLUSIONS, AND RECOMMENDATIONS	52
Summary	52
Conclusions	54
Recommendations	55
LIST OF REFERENCES	57

SECTION PAGE

APPENDIXES 59

A. DATA TRANSFORMATION COMPUTER PROGRAM. 60

B. MATHEMATICAL JUSTIFICATIONS AND DERIVATION OF EQUATIONS . . . 91

VITA 99

LIST OF FIGURES

FIGURE		PAGE
2.1.	Comparison of Results of Simple Compression Tests and Ball Tests to Determine the Yield Stress of Lead Under Impact	9
2.2.	Dynamic Compression Stress-Strain Curve for Commercial Lead Specimens	10
2.3.	Experimental Relation Between Dynamic True Compressive Stress and Compressive Engineering Strain for Pure Lead at Ambient Temperature	12
3.1.	The Specimen Impact Test Facility	16
3.2.	Load Cell and Schematic Diagram of the Instrumentation Used in the Impact Tests	18
3.3.	Load Cell Calibration Curve for Impact Tests	19
3.4.	Schematic Diagram of Apparatus Used to Measure Free-Fall Velocity in Impact Tests	21
3.5.	Quasi-Static True Stress-Strain Curves for Chemical Lead Test Specimens in Compression	23
3.6.	Quasi-Static True Stress-Strain Curves for Chemical Lead Test Specimens in Tension	24
4.1.	Sixty-Eight Specimens After Impact Tests and Five Specimens Not Impacted	26
4.2.	Specimens Before and After Impact Tests	27
4.3.	Typical Force-Time Photograph Taken During Impact Test	29
5.1.	Free-Body Diagram of Weight, Specimen, and Load Cell	33

FIGURE PAGE

5.2. Assumed Curve of Acceleration With Respect to Time 36

5.3. Incrementally Averaged Stress-Strain Data 42

5.4. Stress-Strain Curves for Four Strain-Rate Ranges 43

5.5 Stress-Strain Data Coupled in Ascending Order of Average Strain Rate 44

5.6. Log-Log Plot of $\sigma_t - k$ Versus ϵ 48

5.7. Plot of Equation 5.31 Compared With Plot of Experimental Data 49

5.8. Curves of True Stress and Dynamic Engineering Stress as a Function of Engineering Strain Plotted from Equations Derived from Impact Test Data 51

6.1. Comparison of Plots of Empirical Equation 5.31, Equation 2.8, and Equation 2.9 53

1. INTRODUCTION

The increasing use of radioactive materials for power generation, research, and other applications has necessitated the use of public transportation systems and facilities for the shipment of these materials. To protect the general public and safeguard the surrounding real estate, the Federal Government, through the United States Atomic Energy Commission and the Department of Transportation, has established regulations governing these shipments. These regulations appear as Part 71 of Title 10 of the Code of Federal Regulations (1)*. A portion of the regulations governs the design and performance of containers in which radioactive materials are shipped. To insure that significant quantities of radioactive material are not released and that radiation doses in excess of specified limits are not encountered even under accident conditions, it is required that a container maintain its effectiveness during and after a specified hypothetical accident. This accident has four major conditions, which are outlined as follows.

1. The package must be subjected to a free drop through a distance of 30 feet onto a flat essentially unyielding horizontal surface, striking the surface in a position in which maximum damage is expected.

2. The first condition is followed by a free drop through a distance of 40 inches, striking in a position in which maximum damage is expected the top end of a vertical cylindrical mild-steel bar mounted

---

*Numbers within parentheses in the text designate numbered references given in the List of References.

on an essentially unyielding horizontal surface. The bar shall be 6 inches in diameter, with the top horizontal and its edge rounded to a radius of not more than 1/4 inch, and of such a length as to cause maximum damage to the package but not less than 8 inches long. The long axis of the bar shall be normal to the surface of the package.

3. Next, the package must be subjected to exposure for 30 minutes within a source of radiant heat having a temperature of 1,475°F and an emissivity coefficient of 0.9 or equivalent. For calculational purposes, it shall be assumed that the package has an absorption coefficient of 0.8. The package shall not be cooled artificially until after the 30-minute test period has expired and the temperature at the center of the package has begun to fall.

4. As the last condition, the package must be immersed in water for 24 hours to a depth of at least 3 feet.

1.1 Demonstrating Compliance With the Regulations

Prior to obtaining permission to ship radioactive material in a particular package or container, the shipper must demonstrate to the regulatory body (the United States Atomic Energy Commission or the Department of Transportation) that the container meets the provisions of the regulations. Full-size and model containers have been subjected to the specified accident conditions to demonstrate their compliance with the regulations. However, this practice is not desirable for economic reasons. Also, it is doubtful that many of the features of a shipping container for radioactive material can be adequately modeled. More

often, the shipper demonstrates compliance with the regulations with an approximate analytical analysis of the container in question.

Shipping containers are of two general types: shielded containers used to transport gamma and/or neutron emitting materials and unshielded containers used to transport non-gamma and/or non-neutron emitters. Most of the existing shielded containers employ lead as a shielding material and are designed primarily for shielding against gamma radiation. In general, these containers consist of an inner and outer shell of steel or stainless steel with the space between the shells filled with cast lead. An impact such as required by the first two conditions of the hypothetical accident would result in significant deformation of a shielded container and a reduction in the effectiveness of the shielding. Also, the seal might fail and release radioactive material.

Analyses of shielded containers have generally resulted in ultra-conservative design in that most of these analyses were based on material properties determined by static tests. However, many materials have impact properties which vary significantly from their static properties. Generally, the stress for a given strain will be higher under impact conditions. Hence, if static properties are used to compute the deformation resulting from the free-fall conditions of the hypothetical accident, a deformation significantly larger than the true deformation will be indicated. Since lead is frequently used as the shielding material in shipping casks, the determination of its stress-strain properties under impact conditions is of importance.

1.2 Determination of Stress-Strain Properties of Lead Under Impact Conditions

The study reported here was undertaken to determine the stress-strain properties of lead under impact conditions, and the first step taken was a review of the available technical literature on the subject. It was found that previous work on this subject did not fully fill the needs of the problem being studied, and the decision to conduct an experimental investigation was made. The composition, geometry, and fabrication method of the test material were selected; and conventional static tests were made on the material to verify its static properties and to provide a basis for comparing materials of similar but varying composition. Sixty-eight test specimens were then impacted under simulated accident conditions, and the force-time data were successfully measured and recorded photographically. A computer program was written to transform the test data into stress-strain data, and the results were evaluated.

The findings of the literature search are discussed in Section 2. Development of the test program and apparatus is discussed in Section 3, performance of the tests is described in Section 4, and transformation of the resulting test data and its evaluation are discussed in Section 5. A summary of the test procedures, the conclusions drawn from the results of the tests, and recommendations for future work are presented in Section 6.

2. REVIEW OF LITERATURE

The literature pertaining to the experimental determination of dynamic stress-strain relationships for metals was surveyed for two reasons. The first of these was to determine whether dynamic stress-strain data that could be used to improve the accuracy of the approximate calculation associated with the impacts specified in the first two conditions of the hypothetical accident had been previously developed and published. The second reason was to study the experimental techniques and methods that have been used to obtain similar data.

Hard spheres were dropped on large specimens of ductile materials in experimental investigations conducted by Tabor (2). It was assumed that the concept of a constant dynamic yield pressure, or flow pressure as it was also called, offers a reasonable representation of the actual forces involved in a plastic impact. Tabor derived the expression

$$P = \frac{mg}{\nu}(h_1 - 3h_2) \tag{2.1}$$

for dynamic yield pressure where

P = dynamic yield pressure,

m = mass of the sphere,

g = gravitational acceleration,

ν = volume of indentation,

h_1 = height from which the sphere was dropped, and

h_2 = rebound height of the sphere.

Tabor also empirically derived the expression

$$\sigma_y = \frac{P_s}{K} \tag{2.2}$$

where

σ_y = yield stress of the material,

P_s = static yield pressure, and

K = a constant (called Tabor's constant) found by Tabor (2) to be equivalent to 2.8 for most materials.

Equation 2.2 is valid for low or quasi static velocities. From this work, Tabor (2) found the ratio of P/P_s to be 1.58 for lead. Using this ratio, Equation 2.2, and a value of 2,000 pounds per square inch for σ_y in Equation 2.2; a dynamic yield pressure was computed as follows.

$$P = 1.58P_s = 1.58K\sigma_y \tag{2.3}$$

$$= 8{,}850 \text{ pounds per square inch.}$$

A series of tests similar to those performed by Tabor was conducted in earlier work by Vincent (3). Hard steel spheres were dropped on massive lead specimens in these tests. The diameters of the spheres used were 0.500 inch, 1.000 inch, and 1.500 inches; and the velocity of approach varied from about zero to approximately 45 feet per second. The equation for the dynamic flow pressure developed in this work was

$$P = \frac{16mD}{\pi}\left(\frac{V^2}{d^2}\right) \tag{2.4}$$

where

P = dynamic flow pressure,

m = mass of the sphere,

D = diameter of the sphere,

V = velocity at impact, and

d = diameter of the resulting dent in the lead.

Values of P in the range of 8,700 to 16,850 pounds per square inch were reported.

Similar experiments were conducted by Crook (4). These tests differed from Tabor's (2) in that the specimen was attached to a long lead bar suspended horizontally with a piezoelectric crystal between the specimen and the bar. A freely swinging ball or cylinder was used to impact the specimen. The crystal was calibrated and its output fed to an oscilloscope to record a force-time history of the impact. Crook made simplifying assumptions to interpret his test data. The most important of these was the assumption that the mean pressure over the contact area remains constant throughout the plastic portion of the impact. Dynamic flow pressures in the range of 12,800 to 13,900 pounds per square inch were reported for velocities of approach of 23.25 feet per second.

Dynamic tests in which lead specimens were impacted by hardened steel spheres were conducted by Mok and Duffy (5,6), who also performed static indentation tests of spheres on lead. A series of simple compression tests with both a Hopkinson Bar apparatus and a static compression testing machine were made in conjunction with the sphere-on-lead impact tests, and the results were compared. Spheres with diameters of 1/2 and 1 inch were used in the dynamic impact tests at velocities up to approximately 17 feet per second. Mok and Duffy found Tabor's constant for lead, K, to be 3.59 rather than the 2.8 value determined by Tabor. The flow pressure was computed by using the equation

$$P = \frac{1}{2\alpha}\left(\frac{1}{2}mv^2\right)\frac{\pi d^4}{32D} , \tag{2.5}$$

where

P = dynamic yield pressure,

α = constant = 0.44 to 0.47,

m = mass of sphere,

v = velocity of sphere prior to impact,

d = diameter of the dent in the lead, and

D = diameter of sphere.

The flow pressure (dynamic yield pressure) was converted to stress by using Tabor's (2) equation for static yield pressure in a dynamic sense,

$$\sigma_y = \frac{P}{K} \tag{2.2}$$

with K assigned the value of 3.59. Strain was computed by using the equation

$$\epsilon = \frac{d}{5D} , \tag{2.6}$$

which was also derived by Tabor. Stress was converted to true stress by using the relationship

$$\sigma_t = \text{true stress} = \sigma_y(1 - \epsilon) . \tag{2.7}$$

The equation

$$\sigma_t = b\epsilon^n \tag{2.8}$$

where

b = 7,800 and

n = 0.432

for a strain rate of 150 inches per inch per second for strains up to 0.1 inch per inch was derived from the data resulting from the tests made with the Hopkinson Bar apparatus. The results of the simple compression tests and the ball tests are compared in the plots illustrated in Figure 2.1.

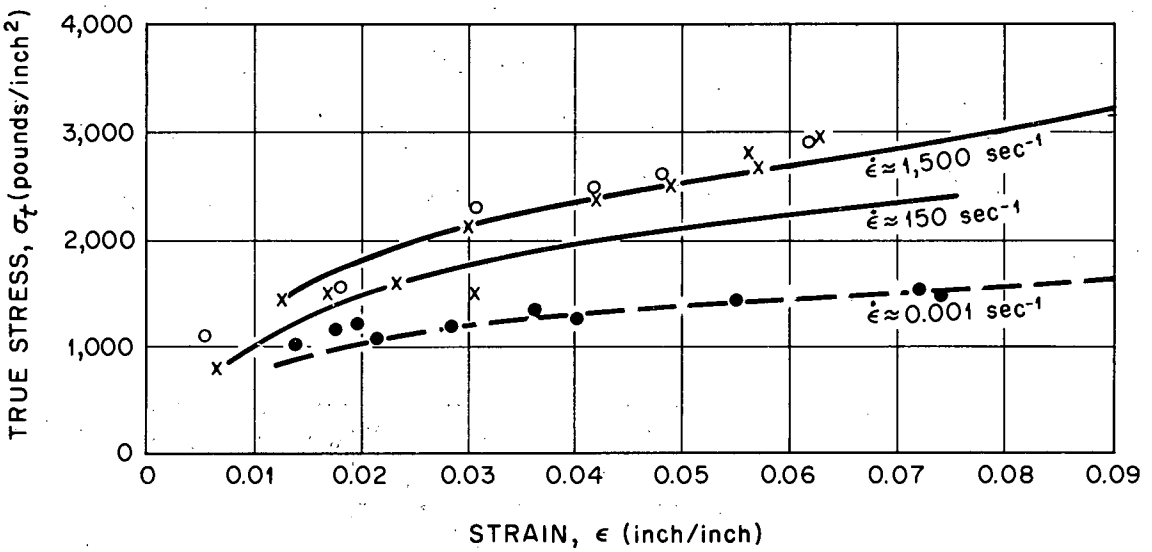

$\dot{\epsilon}$ Strain rate (inch per inch per second)
--- Simple compression tests with static compression machine
—— Simple compression tests with Hopkinson Bar
o Dynamic ball tests with 1/2-inch-diameter steel ball
x Dynamic ball tests with 1-inch-diameter steel ball
● Static ball tests with 1-inch-diameter steel ball

Figure 2.1. Comparison of Results of Simple Compression Tests and Ball Tests to Determine the Yield Stress of Lead Under Impact.

Source: C. H. Mok and J. Duffy, "The Dynamic Stress-Strain Relation of Metals As Determined From Impact Tests With a Hard Ball," International Journal of Mechanical Science (Pergamon Press Ltd., Oxford), Vol. 7, pp. 355-371, 1964.

Experiments with Hopkinson Bar Apparatus were also conducted by Gondusky and Duffy (7). Several specimens of commercial and high-purity lead of various grain sizes and crystallographic orientations were loaded dynamically in compression by means of Hopkinson Bar apparatus. These specimens were right circular cylinders 0.400 inch long with diameters of 0.400 inch. The tests were conducted at strain rates in the range of from 1,100 to 1,200 inches per inch per second. The results of the tests conducted with commercial lead specimens are illustrated in Figure 2.2.

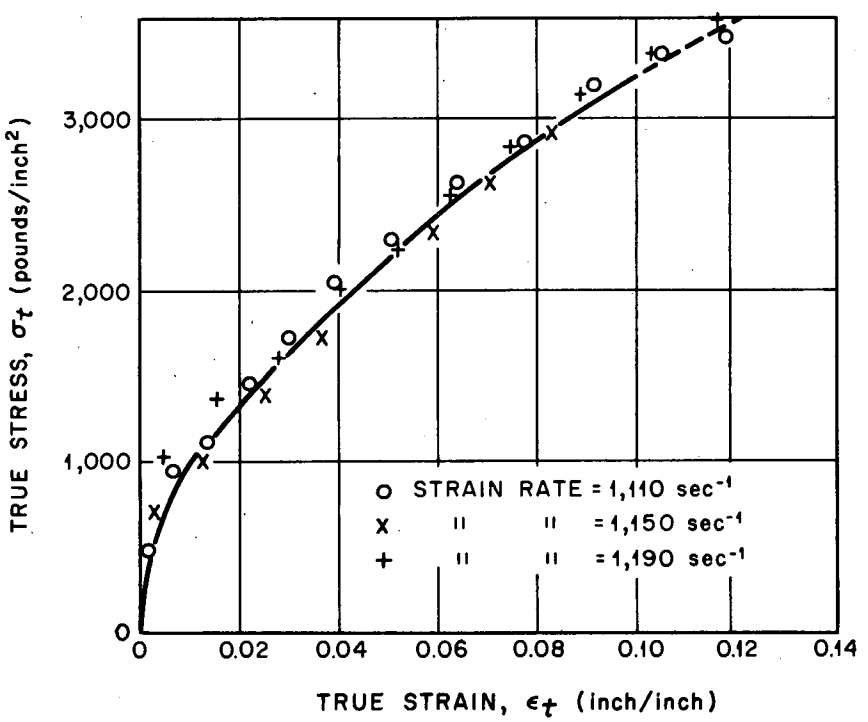

Figure 2.2. Dynamic Compression Stress-Strain Curve for Commercial Lead Specimens.

Source: J. M. Gondusky and J. Duffy, "The Dynamic Stress-Strain Relationship of Lead and Its Dependence On Grain Structure," Technical Report Number 53, Division of Engineering, Brown University, Providence, Rhode Island, May 1967.

Experiments in which right circular cylinders of lead were impacted by a free-falling weight were performed by Slater, Johnson, and Aku (8). The lead specimens were 1 inch long with diameters of 1 inch, and the weight of the falling body was 22.5 pounds. Several drop heights were used, and these ranged from 2 to 12 feet. The free-falling weight did not impact the specimen directly; instead, it impacted a plunger of significant but unreported mass that rested on top of the specimen. The output of a load cell was fed to an oscilloscope to provide a force-time record of each impact. Similarly, a capacitance type of displacement transducer was used in conjunction with the dual-beam oscilloscope to supply a displacement-time history of the impacts. These data enabled the investigators to construct stress-strain curves directly, and the results of their tests are illustrated in Figure 2.3.

In conjunction with their tests, Slater, Johnson, and Aku proposed the approximate equation

$$\sigma_t = \sigma_s(1 + C\dot{\epsilon}^n)K\epsilon^m \tag{2.9}$$

where

σ_t = dynamic true stress,

σ_s = static true compressive stress,

C = constant with mean value of 0.004,

$\dot{\epsilon}$ = average compressive engineering strain rate,

n = index with mean value of 2.02,

ϵ = compressive engineering strain at any instant, and

m = index with mean value of 0.44.

The investigators used Equation 2.9 to predict the results of their experiments to within 15% of the actual test results.

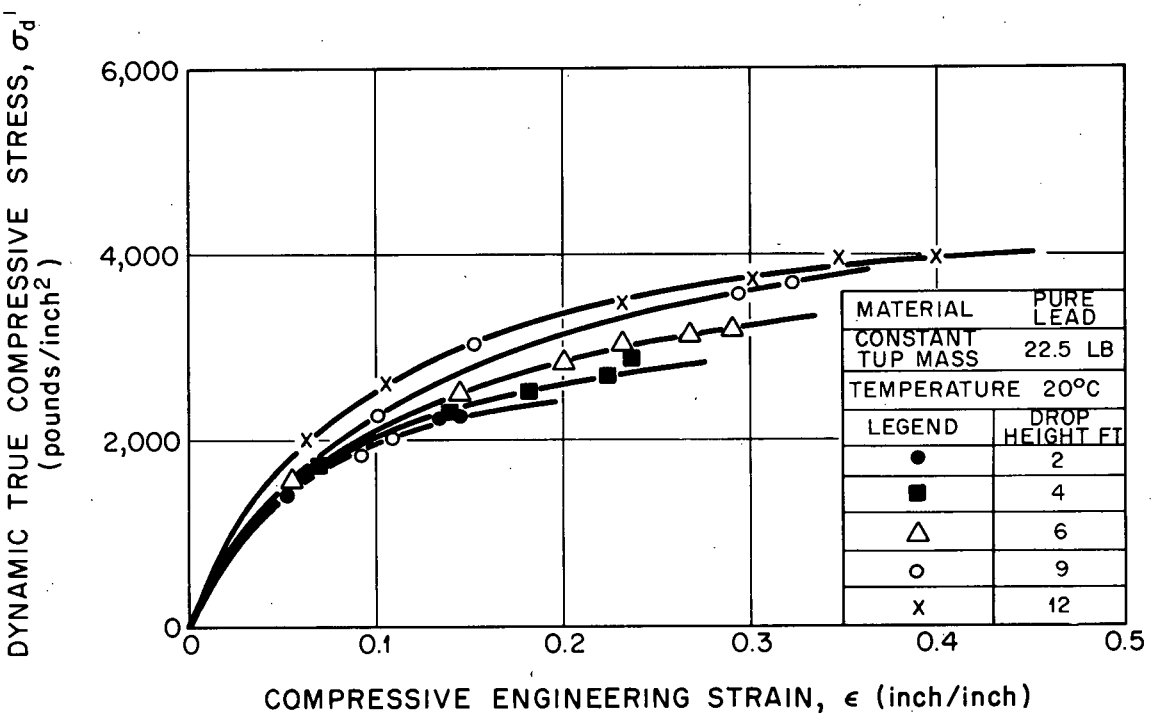

Figure 2.3. Experimental Relation Between Dynamic True Compressive Stress and Compressive Engineering Strain for Pure Lead at Ambient Temperature.

Source: R. A. C. Slater, W. Johnson, and S. Y. Aku, "Experiments in the Fast Upsetting of Short Pure Lead Cylinders and a Tentative Analysis," International Journal of Mechanical Science (Pergamon Press Ltd., Oxford), Vol. 10, pp. 169-186, 1968.

The literature survey revealed that a considerable amount of investigative work has been done to determine the dynamic stress-strain properties of lead and that three unique experimental procedures have been used in this work. The results of the various investigations reported are also correlated within the limits of engineering accuracy. However, the general lack of documentation of the materials tested creates doubt as to what the actual test specimens were in many cases. Also, the maximum strain and impact velocity were limited in most cases. In no sequence of tests reported were strains in excess of 0.2 inch per inch achieved.

3. DEVELOPMENT OF TEST PROGRAM AND APPARATUS

The strain rates used in the investigations of the dynamic stress-strain properties of lead reported in the literature were not generally in the range of those experienced in the 30-foot-free-fall condition of the hypothetical accident. A considerable variation in the results of the investigations reported was also noted. Therefore, it was decided to develop the needed data in an experimental test program.

3.1 Test Philosophy

The general test philosophy of impacting specimens with a free-falling weight was selected as being most applicable to the problem. It was felt that this approach offered the most promising means of obtaining the desired data within the limits of engineering accuracy at a minimum cost. It was also recognized that the successful conclusion of this test program was contingent on being able to measure and record or determine the force applied to the specimen, the velocity of some point or points in the specimen, and the displacement of the specimen with respect to some common function such as time. Considerable difficulty and expense were anticipated if the velocity and displacement were to be measured and recorded directly. In contrast, the techniques for measuring and recording force with respect to time are well developed, universally accepted, and usable at reasonable costs. The other parameters, velocity and displacement, can be derived from the force-with-respect-to-time data.

Force may be converted to acceleration by Newton's Second Law. Acceleration with respect to time may be converted to velocity with respect to time by using the expression

$$v_t = v_o - \int_{t=o}^{t=t} a \, dt, \tag{3.1}$$

where

v_t = velocity at a point in time,

v_o = velocity at time equal to zero, and

a = acceleration.

Similarly, displacement with respect to time may be determined by using the expression

$$X_t = \int_{t=o}^{t=t} v_t \, dt = \int_{t=o}^{t=t} v_o \, dt - \int_{t=o}^{t=t} \int_{t=o}^{t=t} a \, dt \tag{3.2}$$

where X_t = the displacement at a point in time. Additional data, such as stress, true stress, strain, and strain rate, can be determined from these parameters through application of basic engineering disciplines.

3.2 Design of Test Facility and Instrumentation

The test facility shown in Figure 3.1 was designed, fabricated, and installed at the Oak Ridge National Laboratory Drop Tower. Three mild-steel rods 1/2 inch in diameter were suspended the length of the tower and aligned with respect to each other by spacers located at appropriate intervals. This assembly served as a guide for the cylindrical weights used to impact the specimens. The weights consisted of three right circular mild-steel cylinders that weighed 6.94, 8.69, and 10.56 pounds.

PHOTO 98352 A

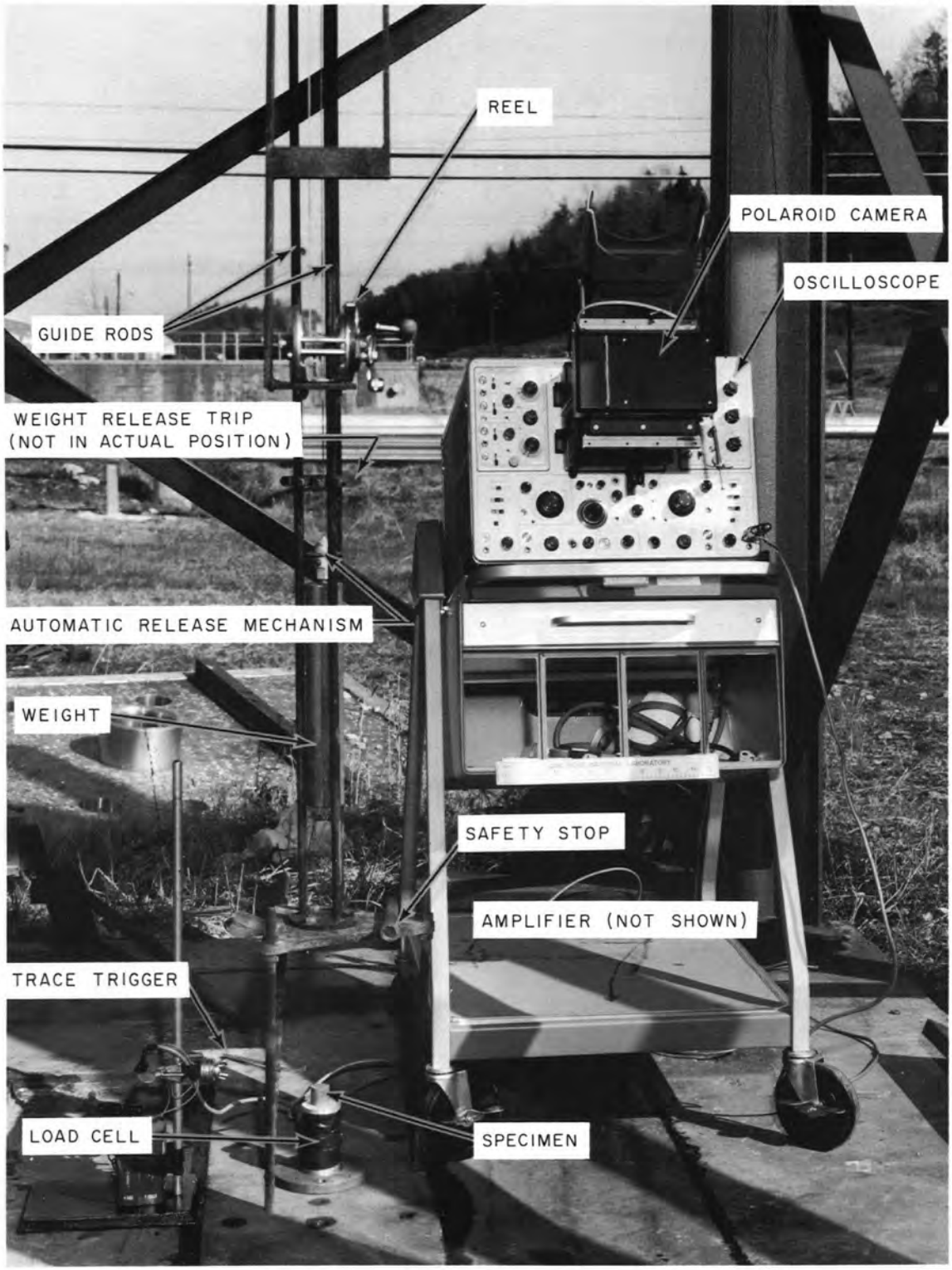

Figure 3.1. The Specimen Impact Test Facility.

The maximum drop height was 432 inches. A spring-loaded ball-detent pin was modified to serve as an automatic release mechanism for the weight to be dropped, and a heavy-duty fishing reel was installed to hoist the weight up to the drop position.

The load cell was designed as a cylinder 4 inches long with an outside diameter of 2 inches and an inside diameter of 1.8 inches and was fabricated of Type 6061-T6 aluminum alloy. Bonded resistance strain gages were cemented to the cell in a full bridge, as illustrated in Figure 3.2. This arrangement effects an approximate two and six-tenths gage output amplification, as compared with a single compression gage. Self-compensating foil gages with a gage length of 1/8 inch were used. The output of the Wheatstone bridge was fed to a Tektronix Type 551 cathode ray oscilloscope after amplification by a Honeywell Model 130-2C amplifier and bridge balance unit. The battery powered trace trigger was selected to initiate the single-sweep scope trace, and a Polaroid camera was used to record the force signal displayed on the screen of the scope at a known sweep rate. A schematic diagram of this apparatus is illustrated in Figure 3.2.

3.3 Instrument Calibration and Preliminary Test

The load cell, amplifier, and oscilloscope package were calibrated to the design capacity of the cell (12,000 pounds) by using a Baldwin 120,000-pound hydraulic compression testing machine. The calibration curve is illustrated in Figure 3.3.

A test was conducted to determine the effect of the guide rods on the free-fall velocity of the weights. The apparatus schematically

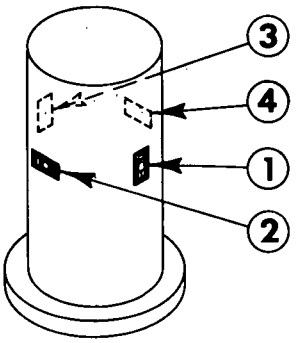

(a) LOAD CELL

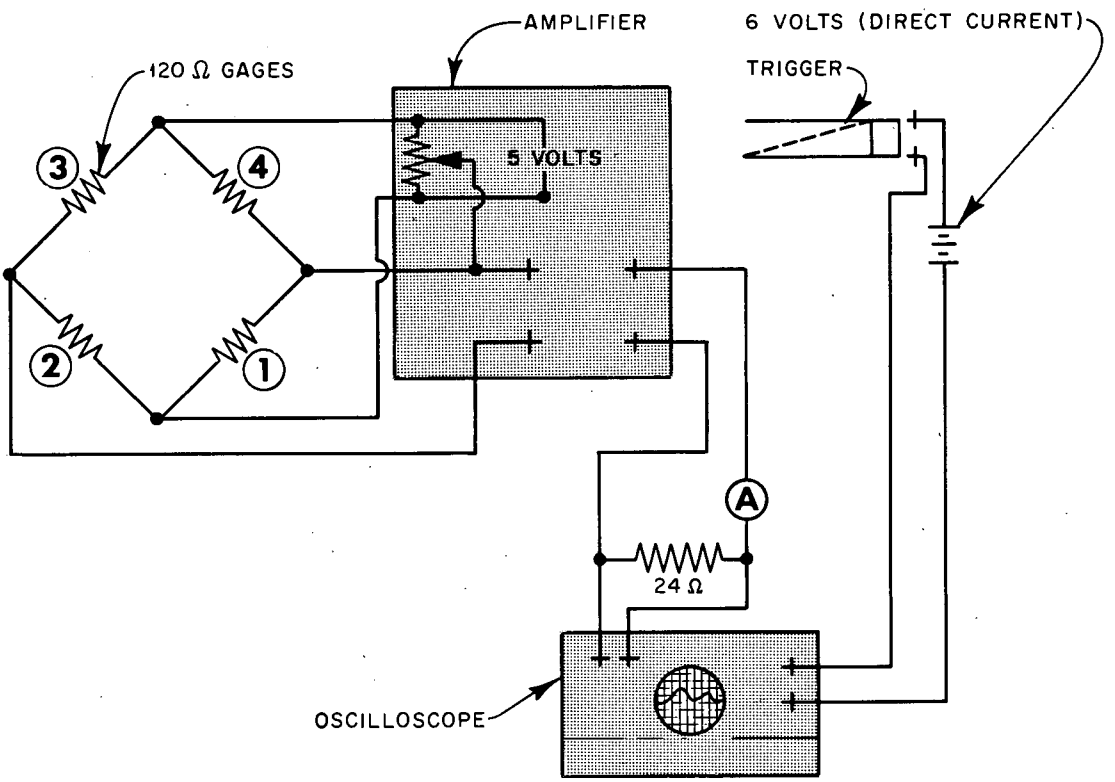

(b) INSTRUMENT SCHEMATIC

Figure 3.2. Load Cell and Schematic Diagram of the Instrumentation Used in the Impact Tests.

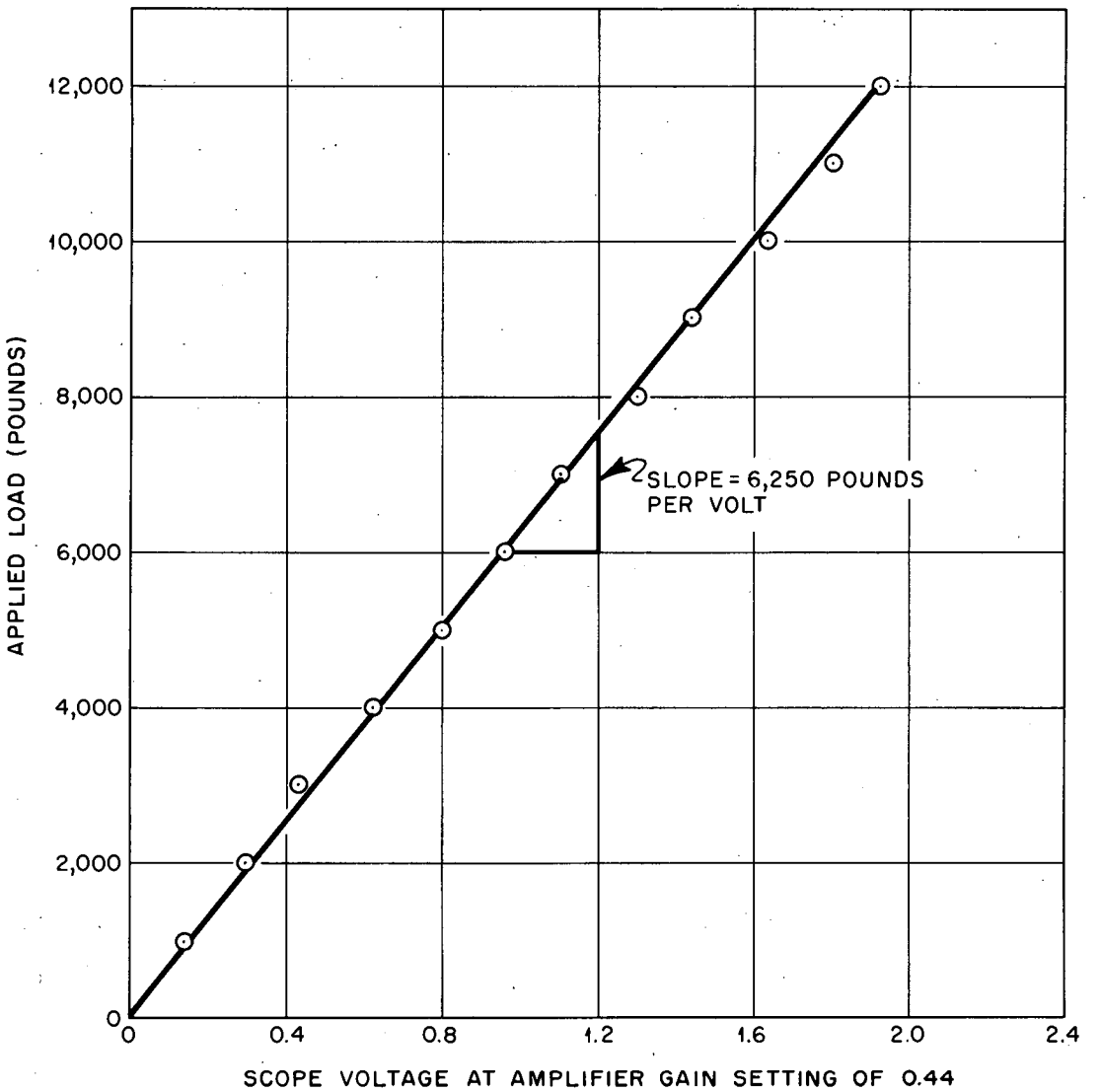

Figure 3.3. Load Cell Calibration Curve for Impact Tests.

illustrated in Figure 3.4 was used to conduct this test. A weight was released from a known elevation. When the falling weight severed the first small conductor, both traces of the dual-beam oscilloscope were initiated. When the second and third conductors were severed, the traces were interrupted. The traces were photographed, as previously described. With the distance between the second and third conductors known and the time required for the weight to travel this distance determined from the photographs, the velocity of the weight at the mid-point between the conductors was computed by using the expression

$$v = \frac{X}{t} \tag{3.3}$$

where

v = velocity,

X = distance, and

t = time.

During this test, weights were released from nominal elevations of 10, 20, and 30 feet. The distance X was held constant at 17.5 inches. The values of velocity determined in this manner deviated a maximum of 0.5% from those computed with the well-known theoretical expression

$$v = (2gh)^{1/2} \tag{3.4}$$

where

g = gravitational constant taken as 32 feet per second per second, and

h = the height or elevation from which the weight falls.

This small deviation indicated that the error introduced into the final results by using the theoretical or ideal free-fall velocity was not significant.

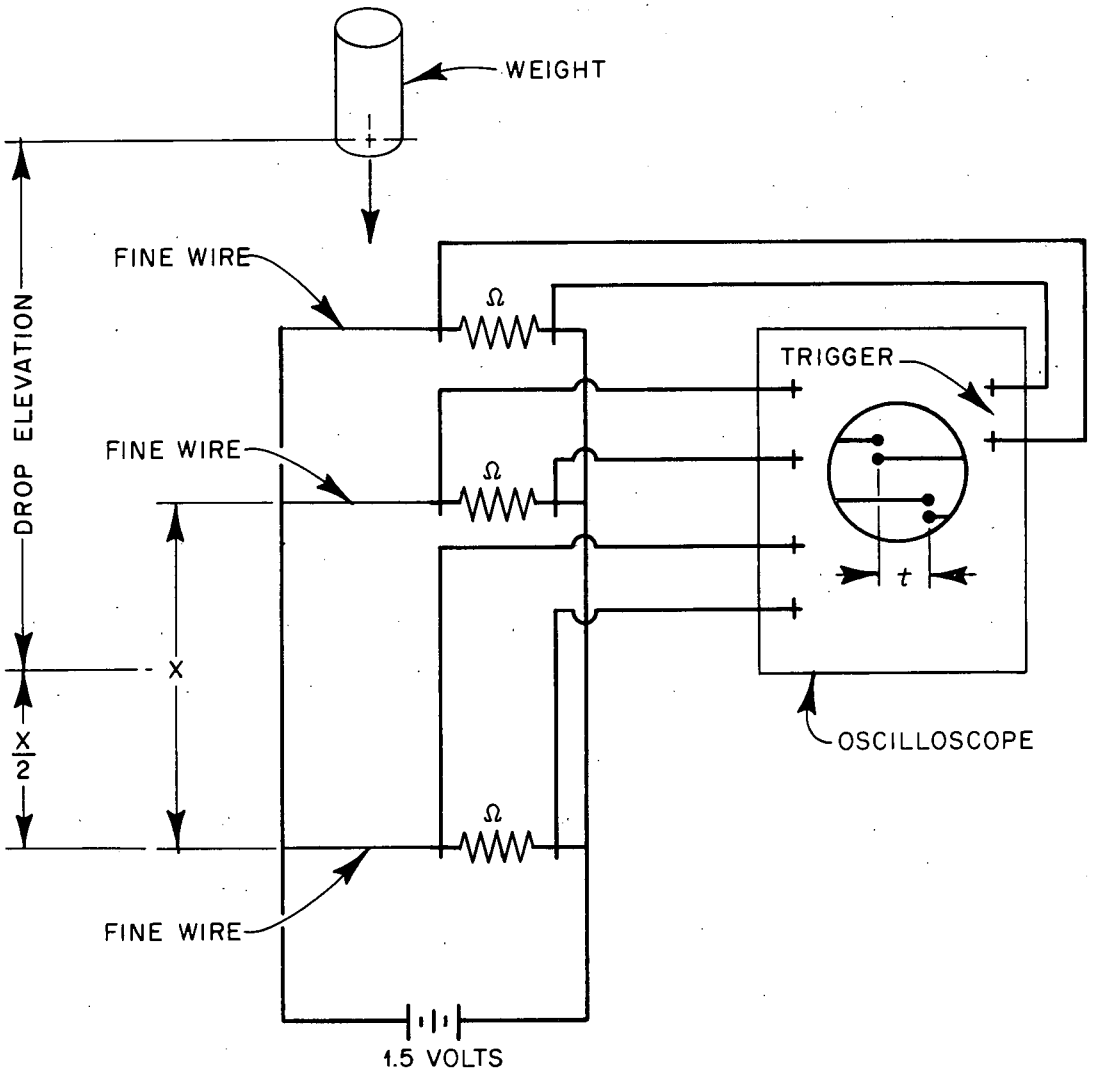

Figure 3.4. Schematic Diagram of Apparatus Used to Measure Free-Fall Velocity in Impact Tests.

3.4 Selection of Test Material and Fabrication of Specimens

A survey of shipping cask design practice revealed that cast-in-place chemical lead was generally specified as the shielding material. The American Society for Testing and Materials Specification ASTM B29 was also frequently used to further specify the material. Chemical lead conforming to ASTM B29 was therefore selected as the test material.

Right circular cylinder impact test specimens with diameters of 1 and 1 1/4 inches and length-to-diameter ratios of 1, 1.5, and 2 were cast in high-quality graphite molds. The ends were machined so that they were parallel to each other and perpendicular to the center line of each cylinder within 0.001 inch in 4 inches. The diameters did not require machining.

Similar static tension and compression test specimens were also fabricated from the same lot of material. Tensile and compressive stress-strain tests were conducted to establish the actual static properties of the impact test material, and the results of these tests are illustrated in Figures 3.5 and 3.6.

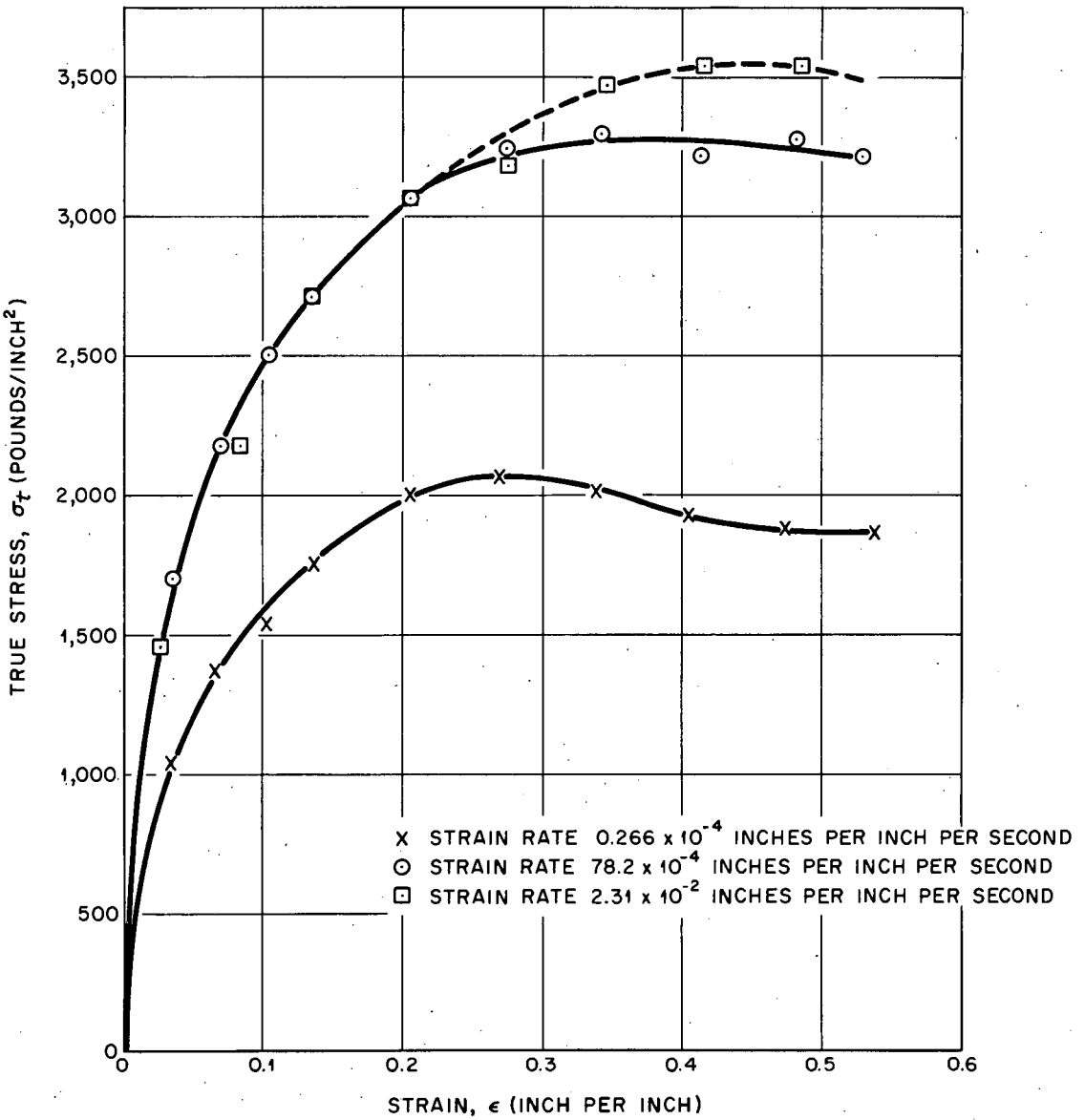

Figure 3.5. Quasi-Static True Stress-Strain Curves for Chemical Lead Test Specimens in Compression.

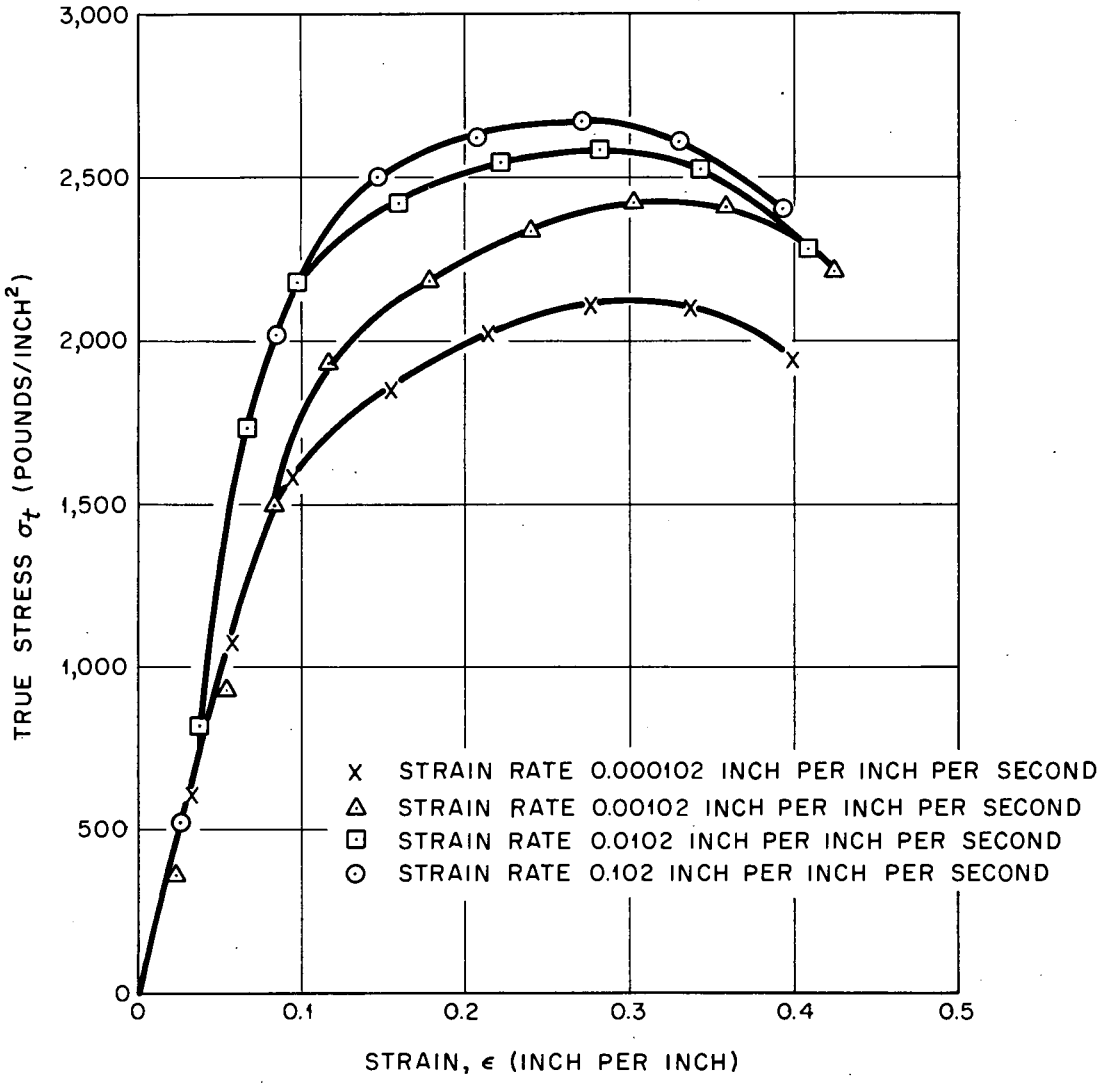

Figure 3.6. Quasi-Static True Stress-Strain Curves for Chemical Lead Test Specimens in Tension.

4. PERFORMANCE OF IMPACT TESTS

Sixty-eight specimens were impact tested, and the force-time data for each impact were successfully measured and photographically recorded with the instrumentation described in Section 3.2 (pages 15-17). Cylindrical lead specimens with five different geometries were tested by using weights of 6.94, 8.69, and 10.56 pounds dropped from several different elevations. Data were taken for the nominal specimen geometry, weight, and drop height combinations given in Table 4.1. Specimens before and after impact tests are shown for visual comparison in Figures 4.1 and 4.2.

Table 4.1

Specimen Geometry, Weight, and Drop Height Combinations Used in Impact Tests

Specimen Geometry		Drop Height in Inches for Weights of		
Diameter (inches)	Length (inches)	6.94 Pounds	8.69 Pounds	10.56 Pounds
1.0	1.0	434.0	432.0	
1.0	1.0	364.0	360.0	360.0
1.0	1.0	288.0		288.0
1.0	1.0	207.0		207.0
1.0	1.0	120.0		120.0
1.0	1.5			431.5
1.0	1.5			359.5
1.0	1.5			240.5
1.0	1.5			120.0
1.0	2.0			359.0
1.0	2.0			240.0
1.25	1.25	359.8		120.0
1.25	2.50			430.5
1.25	2.50			358.5
1.25	2.50			239.8

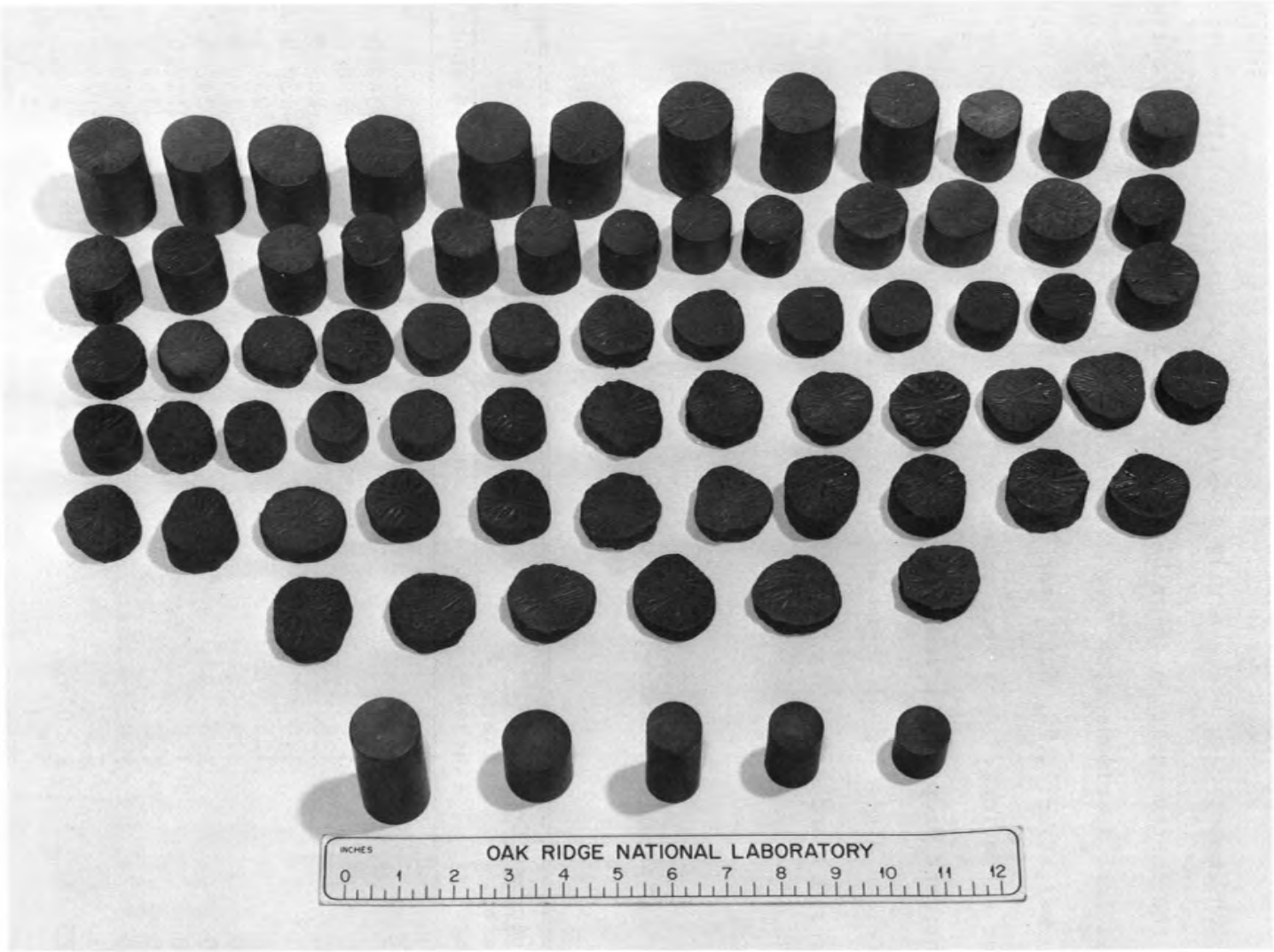

Figure 4.1. Sixty-Eight Specimens After Impact Tests and Five Specimens Not Impacted.

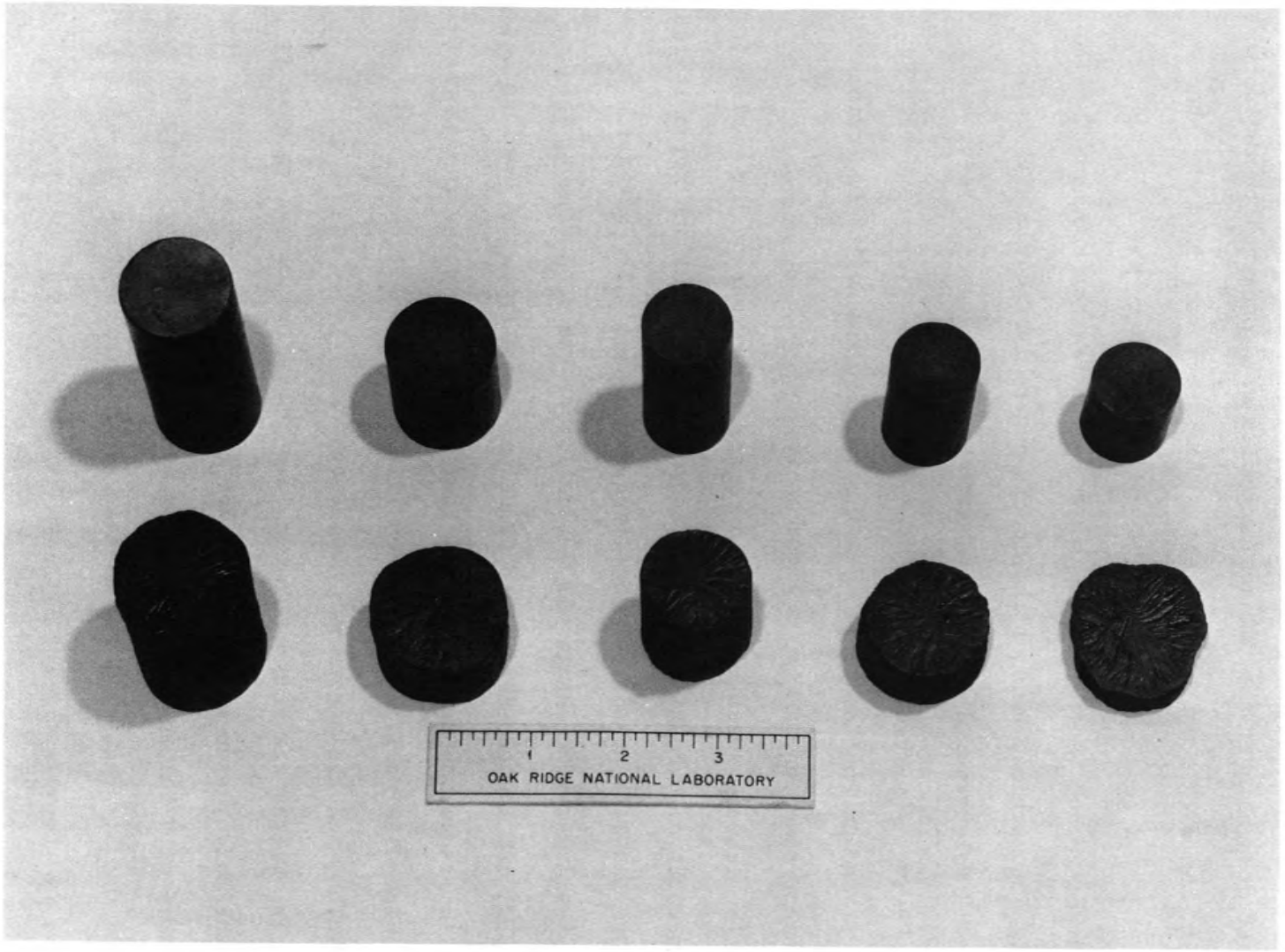

Figure 4.2. Specimens Before and After Impact Tests.

The procedures used to conduct the impact tests for each of the 68 specimens were as follows. The weight release trip was set at the desired drop height, the release mechanism was connected to the selected weight, the weight was hoisted above the safety stop, and the stop was installed. A test specimen of the desired geometry was selected, and its diameter and length were measured to the nearest thousandth of an inch. The machined ends of the specimen were lubricated with Garlock "Luball" molybdenum disulfide high-pressure lubricant to reduce friction between the weight, specimen, and load cell. The specimen was then placed on the load cell and visually centered with the scribed alignment rings on the top surface of the cell.

The desired sweep rate and force scale were set on the oscilloscope. Sweep rates of 0.2 and 0.5 millisecond per centimeter and force scales of 2080 and 3125 pounds per centimeter were used. The selection of the sweep rate and force scale was a function of the drop height, weight dropped, and the geometry of the specimen. The trace trigger was set a small distance, approximately 1/4 to 1/2 inch, above the top of the specimen. The oscilloscope screen illumination was turned to its maximum value, and the screen was photographed.

The weight was hoisted to within a few inches of the release trip and the safety stop was removed. The Polaroid camera was set for time exposure with the scale illumination off and the shutter open. Then the weight was hoisted until the release mechanism contacted the trip, releasing the weight. The free-falling weight first contacted the trace trigger, initiating the single-sweep trace. The falling weight then contacted the specimen and transmitted force to the load cell. As

the specimen deflected and load was applied to the cell, the previously balanced Wheatstone Bridge became unbalanced. The current flow was amplified and fed to the scope through the resistor. This effected a change in the scope voltage that deflected the beam by an amount proportional to the load. The load change with respect to time appeared on the film as a curve, as shown in Figure 4.3.

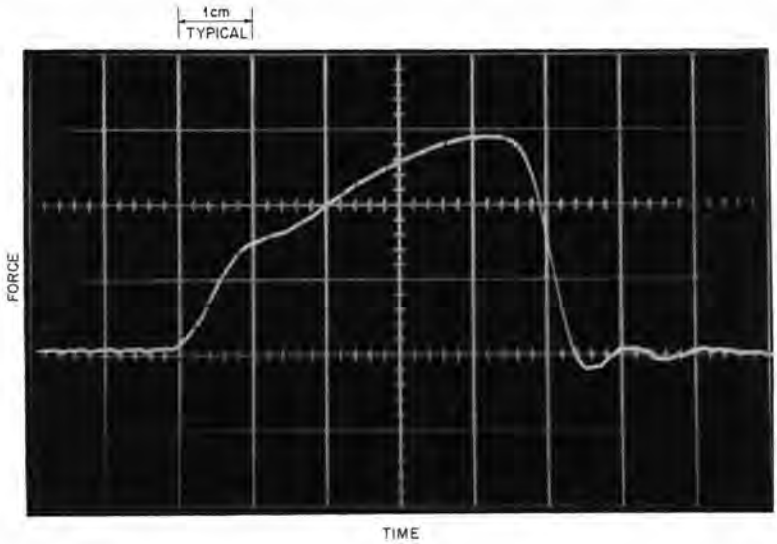

Figure 4.3. Typical Force-Time Photograph Taken During Impact Test.

The impacted specimen was then removed, cleaned, identified by number, and its deformed length measured to the nearest thousandth of an inch and recorded. The force-time photograph was also identified by number, and the scope and amplifier settings were recorded. The weight used to impact the specimen was recorded, and the free-fall distance was measured and recorded. The weights were weighed to the nearest hundredth of a pound prior to testing. These test and data recording procedures were repeated without significant deviation for all of the specimens.

After concluding the impact tests, values of applied force were scaled from the photographs for a constant time increment of 0.1 millisecond. The time required for the impacts varied from a minimum of 1.3 to 2.5 milliseconds. Thus, between 13 and 25 data points with non-zero values were taken for each specimen. The maximum force recorded was approximately 12,000 pounds.

5. DATA TRANSFORMATION AND EVALUATION

The force-time data recorded during the impact tests were transformed into stress-strain data by means of a computer program, and the resulting data were evaluated analytically.

5.1 The Computer Program

A Fortran program applicable to the IBM 360 computer was written to transform the force-time data read from the Polaroid photographs into stress-strain data. The computer program was coded to separate and list the stress values for strains in increments of 0.025 inch per inch, average the stresses and strains in these strain increments, and compute the standard deviation of both average stress and average strain. The stress and strain values were separated and listed with respect to the strain rate in increments of 20 inches per inch per second and also with respect to the average strain rate. This computer program is given in Appendix A.

The values of force scaled from the photographs made during the impact tests were transferred to IBM data cards as were the test parameters or variables of drop height, weight dropped, initial diameter of specimen, initial length of specimen, and the final deformed length of the specimen. The first portion of the computer program down to and including Statement 650 fulfills the routine function of the input of data, dimensioning of storage, and zeroing the storage. The loops formed at Statements 670 to 700 convert the values of force applied to

the load cell to acceleration of the top of the specimen or the bottom of the weight.

A free-body diagram of the weight, specimen, and load cell is illustrated in Figure 5.1. Summation of the forces acting on the specimen results in the expression

$$F'_{(I,J)} - F''_{(I,J)} - F_{(I,J)} = 0 \ , \tag{5.1}$$

where the subscripted letter I refers to the specimen identification number and the subscripted letter J refers to the data point identification number used in the computer program given in Appendix A.

It was assumed that the acceleration of the specimen with respect to its length varied linearly from a value equal to the acceleration of the weight at its top to zero at its bottom. It was also assumed that the acceleration of the weight did not vary with respect to its length and that the load cell remained stationary. Within the framework of these assumptions, the equation of equilibrium becomes

$$M_w A_{(I,J)} - \frac{M_s A_{(I,J)}}{2} = F_{(I,J)} \ , \tag{5.2}$$

where

M_w = mass of the weight dropped,

A = acceleration in feet per second per second, and

M_s = mass of specimen.

Solving Equation 5.2 for $A_{(I,J)}$ and substituting constants and test parameters for mass results in the expression

$$A_{(I,J)} = \frac{F_{(I,J)} 32.0}{W_{(I)} - \frac{\pi}{8} D^2_{(I)} C_{(I)} \rho} \ , \tag{5.3}$$

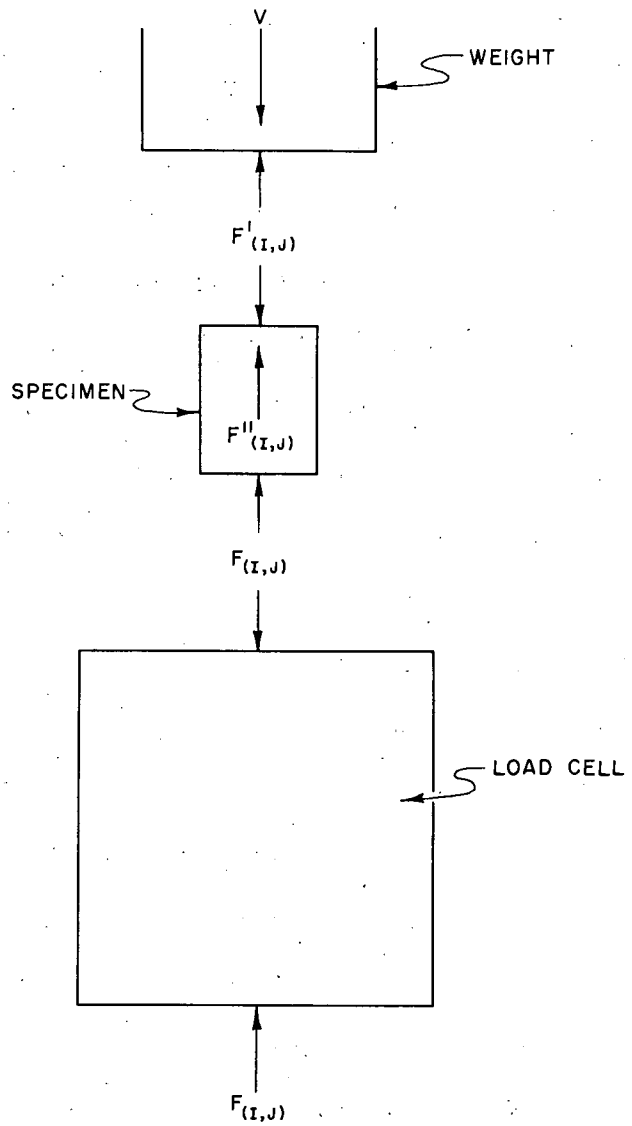

Figure 5.1. Free-Body Diagram of Weight, Specimen, and Load Cell.

where

W = weight of impacting weight in pounds,

D = initial diameter of specimen in inches,

C = initial length of specimen in inches, and

ρ = density of specimen.

Equation 5.3 is equivalent to the Fortran equation in Statement 690 of the computer program after constants have been substituted.

The loops at Statements 710 to 730 in the computer program compute the initial velocity V_o, which is defined as the velocity when time and force equal zero. It was assumed that the velocity of the top of the specimen and the velocity of the bottom of the falling weight are the same and that the velocity of the specimen varies linearly over its length from a maximum at its top surface to zero at its bottom surface. Therefore, the initial velocity of the center of mass of the specimen is one-half the initial velocity. The assumption that if the stress wave has propagated the length of the specimen at this time, the resulting external force applied to the bottom of the specimen is negligible is demonstrated in Appendix B. Within this framework, the principle of conservation of momentum for this system may be stated in conventional mathematical notation as follows.

$$V_o' M_w = V_o M_w + \frac{V_o}{2} M_s \ , \tag{5.4}$$

where

V_o' = velocity of falling weight upon impact,

M_w = mass of weight,

V_o = initial velocity of weight and specimen at $T = 0$, and

M_s = mass of specimen.

Dividing Equation 5.4 through by M_w, substituting $(2gH)^{1/2}$ for V_o', and solving for V_o results in the expression

$$V_{o(I)} = \frac{\left(2gH_{(I)}\right)^{1/2}}{1 + \frac{\pi D^2_{(I)} C_{(I)} \rho}{8W_w}}, \tag{5.5}$$

where

g = gravitational acceleration,

H = drop height of weight in inches,

ρ = density of specimen, and

W_w = weight of dropped weight in pounds.

Equation 5.5 is equivalent to the Fortran equation in Statement 700 of the computer program given in Appendix A.

The loops between Statements 770 and 970 in the computer program convert the acceleration-with-respect-to-time data to velocity-with-respect-to-time data. From basic engineering mechanics it is known that

$$V_{(I,J)} = V_{o(I)} - \int_{t=0}^{t=T} a \, dt \, . \tag{5.6}$$

Since the function for acceleration with respect to time is unknown, the integral cannot be evaluated. However, the value of the acceleration at specific points in time is known, and the integral can be evaluated by approximate numerical integration techniques. Simpson's Rule of numerical integration is such a technique.

The curve shown in Figure 5.2 was assumed to be a plot of acceleration with respect to time with ΔT a constant. For an acceleration-time curve such as this, the application of Simpson's Rule results in the expression

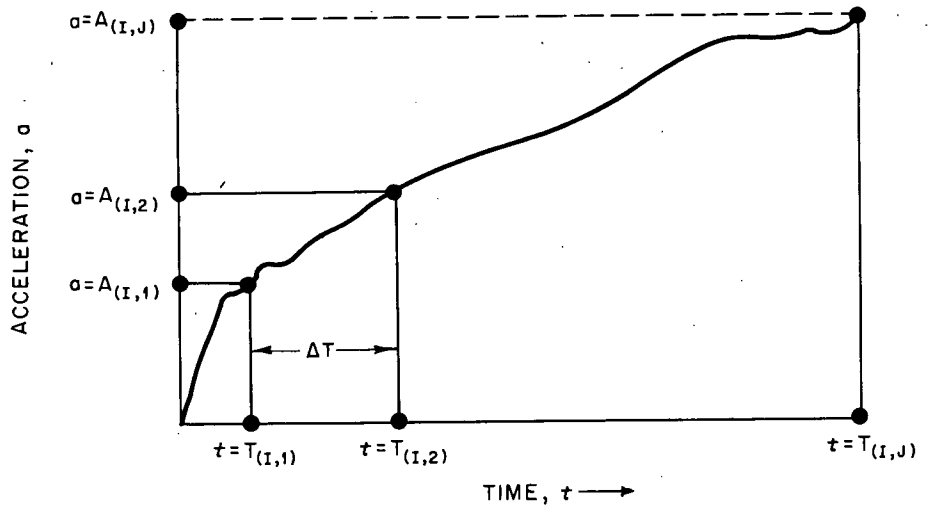

Figure 5.2. Assumed Curve of Acceleration With Respect to Time.

$$V_{(I,J)} = V_{o(I)} - \frac{\Delta T}{3}\Big[A_{(I,0)} + A_{(I,J)} + 4\big(A_{(I,1)} + A_{(I,3)} + \cdots + A_{(I,J-1)}\big) + 2\big(A_{(I,2)} + A_{(I,4)} + \cdots + A_{(I,\ J-2)}\big)\Big] \quad . \quad (5.7)$$

For the data taken in the impact tests, $A_{(I,0)}$ is always zero. This method is limited in that J must be an even integer. However, when J is an odd integer, this limitation can be overcome by computing the area of the first increment by the trapezoidal rule and applying Simpson's Rule to the increments 1 to J. Since it was desirable from an accuracy standpoint to compute the velocity at every data point, this technique was followed. Equation 5.8 is valid for an odd number of increments.

$$V_{(I,J)} = V_{o(I)} - \Delta T\,\frac{\big(A_{(I,0)} + A_{(I,1)}\big)}{2} + \frac{\Delta T}{3}\Big[A_{(I,1)} + A_{(I,J)} + 4\big(A_{(I,2)} + A_{(I,4)} + \cdots + A_{(I,J-1)}\big) + 2\big(A_{(I,3)} + A_{(I,5)} + \cdots + A_{(I,J-2)}\big)\Big] \quad . \quad (5.8)$$

However, Equation 5.8 is not valid for one increment, and the expression

$$V_{(I,1)} = V_{o(I)} - \frac{\Delta T}{2}\left(A_{(I,0)} - A_{(I,1)}\right) \tag{5.9}$$

must be used to evaluate the velocity at the first data point with a non-zero value.

A series of three similar loops located between Statements 1010 and 1210 in the computer program, which is given in Appendix A, evaluates the deformation of the specimen with respect to time. Simpson's Rule is used to numerically integrate the expressions. The previously discussed limitations concerning increments are also applicable in this case, and ΔT is again constant. The expression

$$X_{(I,1)} \cong \Delta T \frac{V_{o(I)} + V_{(I,1)}}{2} \tag{5.10}$$

for one increment where X = deformation of the specimen, the expression

$$\begin{aligned} X_{(I,J)} = \frac{\Delta T}{3}\Big[V_{o(I)} + V_{(I,J)} + 4\big(A_{(I,1)} + A_{(I,3)} \\ + A_{(I,5)} + \cdots + A_{(I,J-1)}\big) \\ + 2\big(A_{(I,2)} + A_{(I,4)} + A_{(I,6)} + \cdots + A_{(I,J-2)}\big)\Big] \end{aligned} \tag{5.11}$$

for an even number of increments, and the expression

$$\begin{aligned} X_{(I,J)} = \Delta T \frac{V_{o(I)} + V_{(I,1)}}{2} + \frac{\Delta T}{3}\Big[V_{(I,1)} + V_{(I,J)} \\ + 4\big(A_{(I,2)} + A_{(I,4)} + \cdots + A_{(I,J-1)}\big) \\ + 2\big(A_{(I,3)} + A_{(I,5)} + \cdots + A_{(I,J-2)}\big)\Big] \end{aligned} \tag{5.12}$$

for an odd number of increments equal to three or more were used to evaluate the deflection at any point in time.

Deflection is converted to strain in the loop formed by Statement 1220 through Statement 1260 of the computer program, which is given in Appendix A. The equation defining strain from elementary strength of materials

$$XE_{(I,J)} = \frac{X_{(I,J)}}{C_{(I)}} , \tag{5.13}$$

where

XE = strain in inches per inch,

X = deformation of specimen in inches, and

C = initial length of specimen in inches;

was used to effect this conversion.

Force is converted to engineering stress in the loop formed by Statements 1280 through 1310 of the computer program. The basic equation for engineering or apparent stress

$$S_{(I,J)} = \frac{F_{(I,J)}}{\frac{\pi D^2_{(I)}}{4}} , \tag{5.14}$$

where

S = engineering stress in pounds per square inch,

F = force in pounds, and

D = initial diameter of the specimen in inches;

is equivalent to the Fortran equation in Statement 1300.

The computation of true stress effected in the loop formed by Statements 1330 through 1360 in the computer program is slightly more complicated since the actual cross-sectional area of the specimen with respect to time is not known. Lead is essentially incompressible, and the volume of the specimen at any point in time is approximately equal

to the initial volume. The expression

$$\frac{\pi D^2_{(I)} C_{(I)}}{4} = \text{Area}_{(I,J)} C_{(I)} \left(1 - XE_{(I,J)}\right) , \tag{5.15}$$

where

D = diameter of specimen in inches,

C = initial length of specimen in inches,

X = deformation of specimen in inches, and

XE = strain in inches per inch;

may be solved for $\text{Area}_{(I,J)}$ and the expression for true stress written.

$$ST_{(I,J)} = \frac{F_{(I,J)} \left(1 - XE_{(I,J)}\right)}{\frac{\pi D^2_{(I)}}{4}} \tag{5.16}$$

where

ST = true stress in pounds per square inch and

F = force in pounds.

The final deformation of the specimen is computed in the loop formed by Statements 1380 through 1410 of the computer program, which is given in Appendix A.

The remainder of the computer program is related to the output of computed variables and grouping of these variables to facilitate interpretation of the data. Statements 1410 through 1431 effect the printing of all computed double-subscripted variables and certain single-subscripted test parameters.

The next three loops from Statements 1470 through 2530 group the stress-strain data by strain increments of 0.025 inch per inch, average the stress and strain over these strain increments, compute the standard

deviation of average stress and average strain, and print this data. The first of these loops performs these operations by using all the test data from all 68 specimens. The second loop uses only that data which accounts for a minimum of 90% of the available kinetic energy, and the third loop uses only that data which accounts for a minimum of 95% of the available kinetic energy. The percentage of the available kinetic energy accounted for is based on the difference between the kinetic energy possessed by the system at time equal zero (when the velocity is equal to the initial velocity) and the kinetic energy indicated by the computed velocity at the last data point (point of maximum force). The Fortran equation in Statement 1920 of the computer program that computes the percentage of kinetic energy accounted for is derived in Appendix B.

The next loop formed by Statements 2540 through 2670 of the computer program groups the true stress and strain values with respect to the strain rate computed in increments of 20 inches per inch per second. The Fortran equation in Statement 2570 that computes strain rate is derived in Appendix B. The loop formed by Statements 2690 through 3100 groups the stress and strain values with respect to the average strain rate in increments of 55 inches per inch per second. The equation in Statement 2700 that computes the average strain rate is derived in Appendix B.

The percentage difference between the measured (maximum) deflection and the computed maximum deflection is determined in the loop formed by Statements 3110 through 3140 of the computer program. The last portion of the program, Statements 3150 through 3680, effects the printout of the input force-time data and all single-subscripted variables and test parameters. This portion of the output is also presented in Appendix A.

5.2 Evaluation of Computer Output

The incrementally averaged stress-strain data are plotted in Figure 5.3. It is noted that the curve plotted from data which accounts for a minimum of 95% of the available kinetic energy exhibits the highest value of stress for a given strain. Similarly, the curve plotted from the data which accounts for a minimum of 90% of the available kinetic energy has higher values of true stress for a given strain than does the curve plotted from the averaged test data for all 68 of the specimens.

It is felt that the data group which accounts for the greatest percentage of the available kinetic energy most nearly represents the real dynamic stress-strain curve for lead. This supposition cannot be proved but can be justified by the fact that this group of data includes 51.5% of the specimens tested and exhibits a significantly lower deviation. The maximum deviation in stress is approximately 1,100 pounds per square inch, and it occurs in the curve plotted from all the data at a strain of 0.5 inch per inch. This amounts to a 20% deviation based on the mean of the stress values at the point of maximum deviation.

Study of the computer printout of stress and strain values grouped in ascending increments of strain rate shows that the true compressive stress for a given strain is not significantly dependent upon the strain rate within the limits of the impact test data. This is illustrated in Figure 5.4 in which stress-strain curves for four selected strain-rate ranges are shown. The stress-strain data grouped in ascending order of average strain rate shown in Figure 5.5 further demonstrate that lead is not significantly rate sensitive within the range of the impact test data. However, comparison of all the experimental dynamic stress-strain

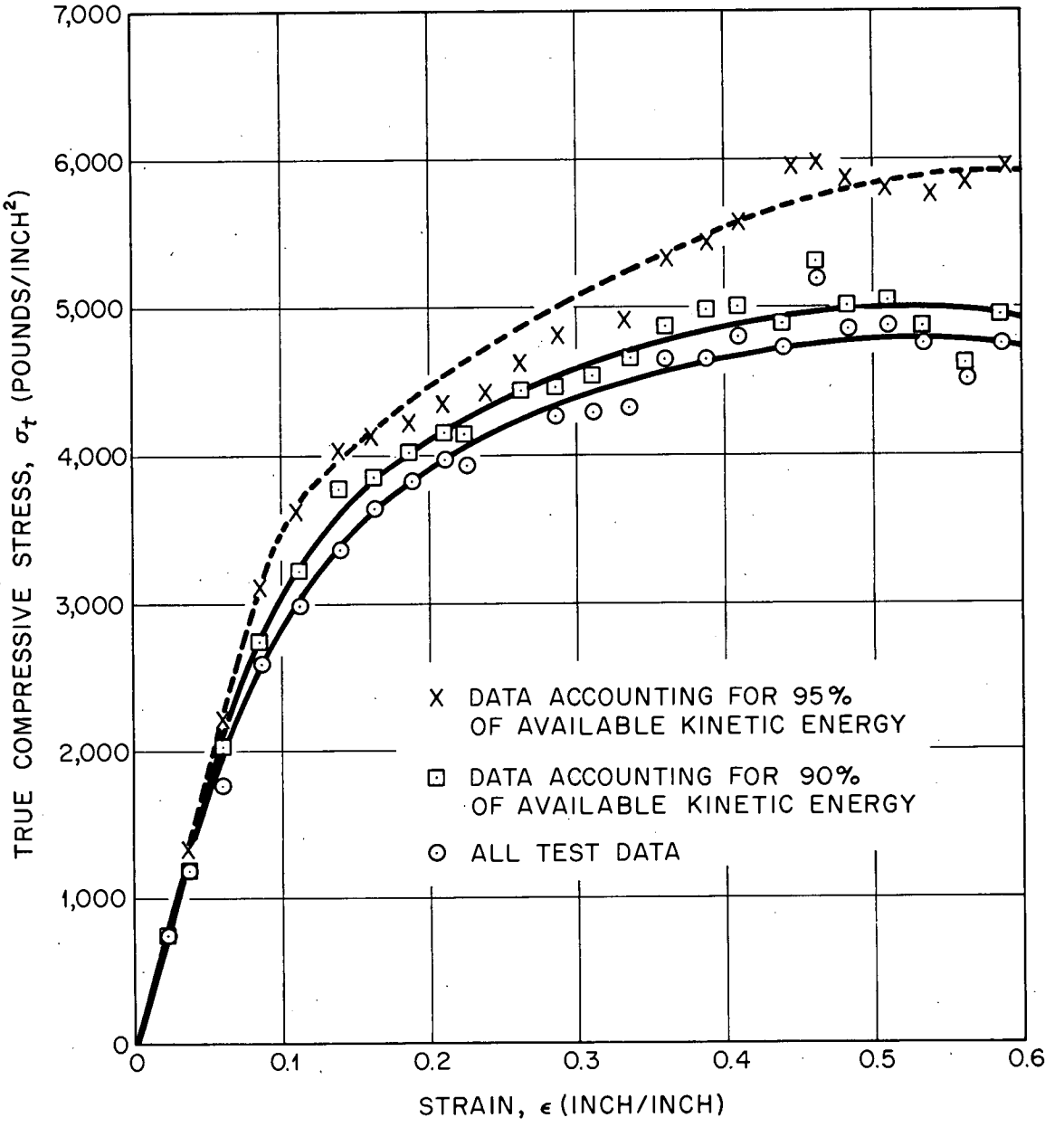

Figure 5.3. Incrementally Averaged Stress-Strain Data.

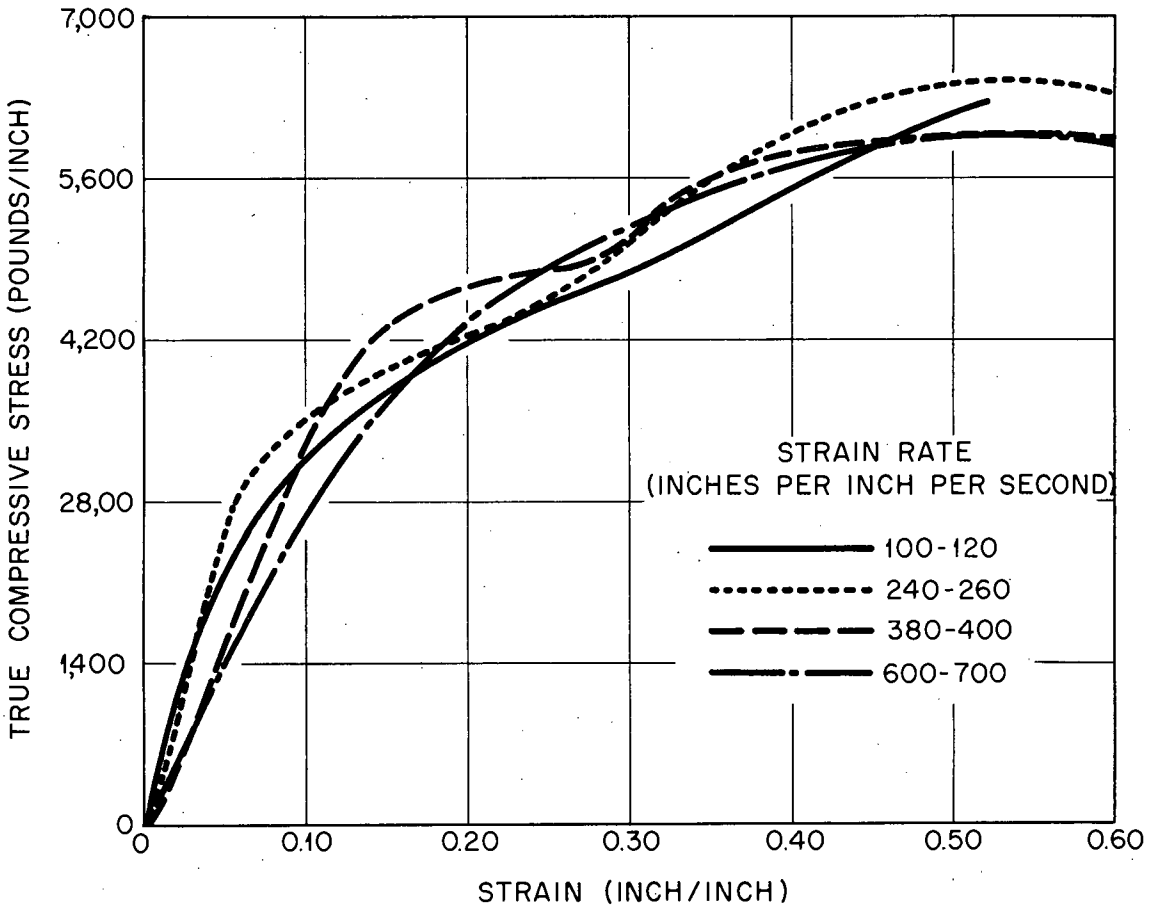

Figure 5.4. Stress-Strain Curves for Four Strain-Rate Ranges.

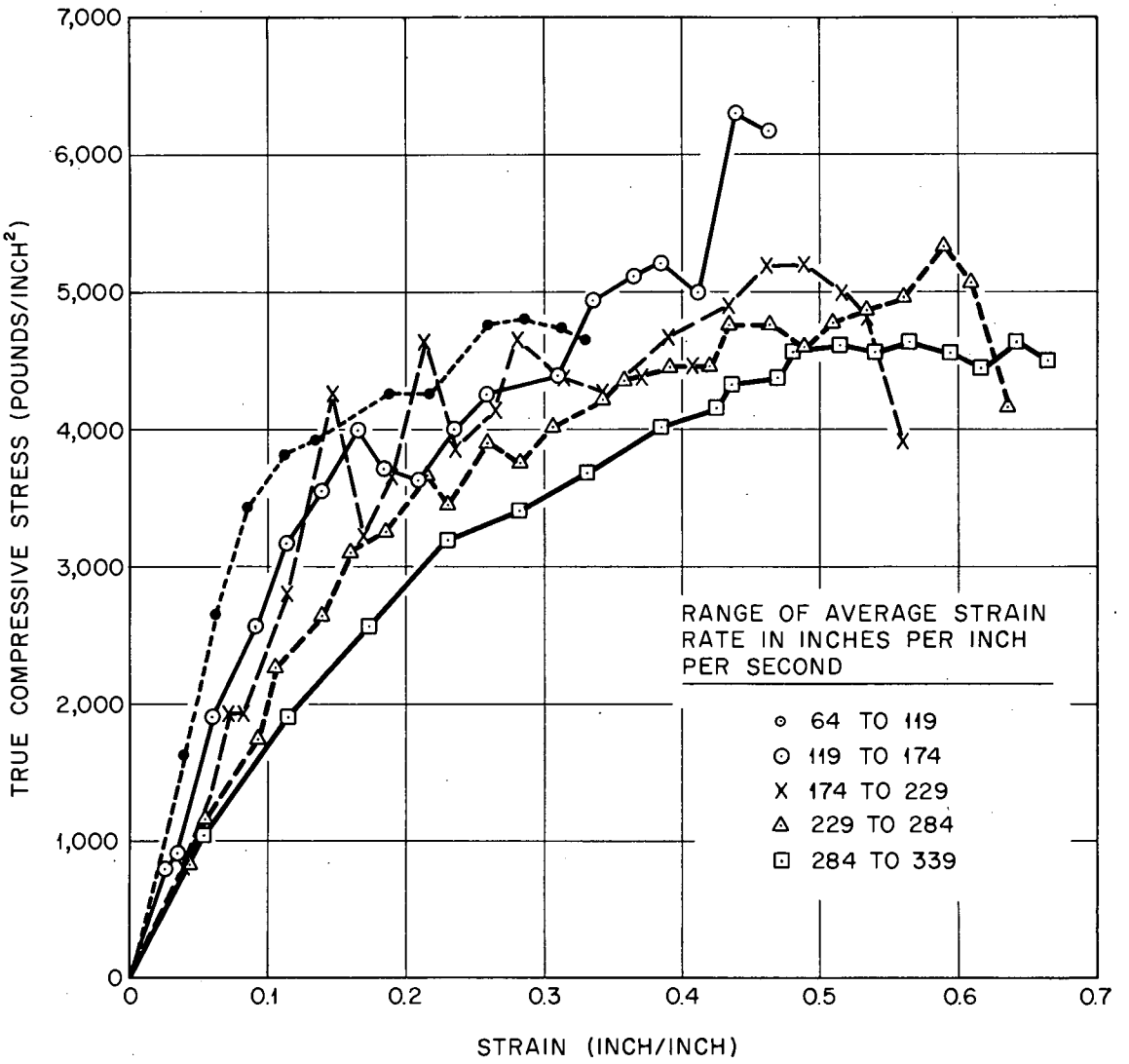

Figure 5.5. Stress-Strain Data Coupled in Ascending Order of Average Strain Rate.

data with static stress-strain data shows that lead is rate sensitive with respect to static or quasi-static strain rates.

An equation of the general form

$$S_t = f(\epsilon) \tag{5.17}$$

describing the applied true compressive stress as a function of strain would be of considerable value in evaluating the effects of the impact conditions specified in the hypothetical accident. Observation of the true stress-strain curve plotted from the impact test data which accounts for a minimum of 95% of the available kinetic energy illustrated in Figure 5.3 (page 42) indicates that an equation of the form

$$\sigma_t = b\epsilon^m + k \ , \tag{5.18}$$

where

σ_t = true compressive stress in pounds per square inch,

b = a constant,

ϵ = strain in inches per inch,

m = an index, and

k = a constant;

possibly describes the experimental impact data adequately. There are numerous accepted procedures for fitting experimental data to equations. The determination of the constants in Equation 5.18 may be accomplished by using the following procedure (9).

The points $(\epsilon_1, \sigma_{t1})$ and $(\epsilon_2, \sigma_{t2})$ are chosen at or near the extremities of the curve formed by the experimental data. The coordinate ϵ_3, which is the geometric mean of the points ϵ_1 and ϵ_2, is computed from the expression

$$\epsilon_3 = [(\epsilon_1)(\epsilon_2)]^{1/2} \ . \tag{5.19}$$

The value of σ_{t_3} may be read from the plot of the curve illustrated in Figure 5.3 (page 42). The points (ϵ_1,σ_{t1}), (ϵ_2,σ_{t2}), and $(\epsilon_3,\sigma_{t_3})$ need not be data points but must lie on the curve formed by the experimental data. Equation 5.18 is rearranged in the form

$$\sigma_t - k = b\epsilon^m , \tag{5.20}$$

and the logarithm of both sides is taken, resulting in the expression

$$\log (\sigma_t - k) = m \log \epsilon + \log b . \tag{5.21}$$

The points (ϵ_1,σ_{t1}), (ϵ_2,σ_{t2}), and $(\epsilon_3,\sigma_{t_3})$ are substituted in Equation 5.21, and the following three equations result.

$$\log (\sigma_{t1} - k) = m \log \epsilon_1 + \log b \tag{5.22}$$

$$\log (\sigma_{t2} - k) = m \log \epsilon_2 + \log b \tag{5.23}$$

$$\log (\sigma_{t_3} - k) = m \log \epsilon_3 + \log b \tag{5.24}$$

Addition of Equations 5.22 and 5.23 results in the equation

$$\frac{\log (\sigma_{t1} - k)(\sigma_{t2} - k)}{2} = m\left(\frac{\log \epsilon_1 + \log \epsilon_2}{2}\right) + \log b \tag{5.25}$$

Division of Equation 5.25 by Equation 5.24 results in the equation

$$\frac{\log (\sigma_{t1} - k)(\sigma_{t2} - k)}{2(\log \sigma_{t_3} - k)} = \frac{m\left(\frac{\log \epsilon_1 + \log \epsilon_2}{2}\right) + \log b}{m \log \epsilon_3 + \log b} . \tag{5.26}$$

Substituting $[(\epsilon_1)(\epsilon_2)]^{1/2}$ for ϵ_3, Equation 5.26 reduces to

$$\frac{\log (\sigma_{t1} - k)(\sigma_{t2} - k)}{2 \log (\sigma_{t_3} - k)} = 1 \tag{5.27}$$

or

$$\log (\sigma_{t1} - k)(\sigma_{t2} - k) = 2 \log (\sigma_{t_3} - k) . \tag{5.28}$$

Taking the logarithm of both sides of Equation 5.28 and solving for k results in the equation

$$k = \frac{\sigma_{t_1}\sigma_{t_2} - \sigma_{t_3}^{2}}{\sigma_{t_1} + \sigma_{t_2} + \sigma_{t_3}^{3}} \tag{5.29}$$

from which k may be evaluated. A plot of $\sigma_t - k$ versus ϵ is made on log-log paper, approximating a straight line having the equation

$$\sigma_t = b\epsilon^m + k \ . \tag{5.18}$$

The constants b and m may be evaluated from this graph where b is the σ intercept at $\epsilon = 1$ and m is the slope of the line, and the equation for true stress may be written. This equation may then be converted to an equation for engineering stress by using the relationship

$$\sigma_e = \frac{\sigma_t}{1 - \epsilon} = \frac{1}{1 - \epsilon}(b\epsilon^m + k) \ . \tag{5.30}$$

Following the procedure just discussed, the points (0.0021, 718) and (0.52, 5900) were selected from the curve plotted from the experimental data accounting for a minimum of 95% of the available kinetic energy that is illustrated in Figure 5.3 (page 42). These points fulfill the requirement that they be near the extremities of the curve. The value of σ_{t_3} was then read from the curve as being 3,500 pounds per square inch. The constant k was computed from Equation 5.29 and found to be 20,980. The constants b and m were determined from the plot of σ_t - k versus ϵ shown in Figure 5.6. The value of the constant b was found to be 14,250, and the value of m was found to be -0.093. Hence, the equation

$$\sigma_t = 20{,}980 - 14{,}250\epsilon^{-0.093} \tag{5.31}$$

describes the dynamic true stress-strain curve for lead. The curve of this equation demonstrates reasonable agreement with the experimental data at strains up to 0.5 inch per inch, as is shown in Figure 5.7.

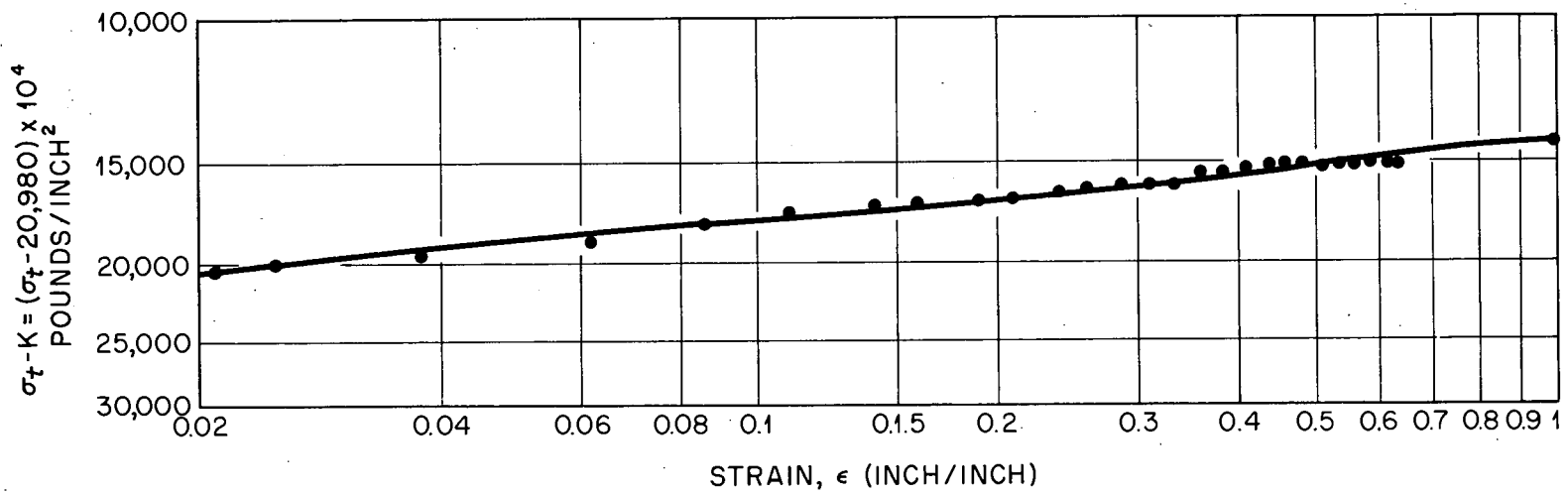

Figure 5.6. Log-Log Plot of $\sigma_t - k$ Versus ϵ .

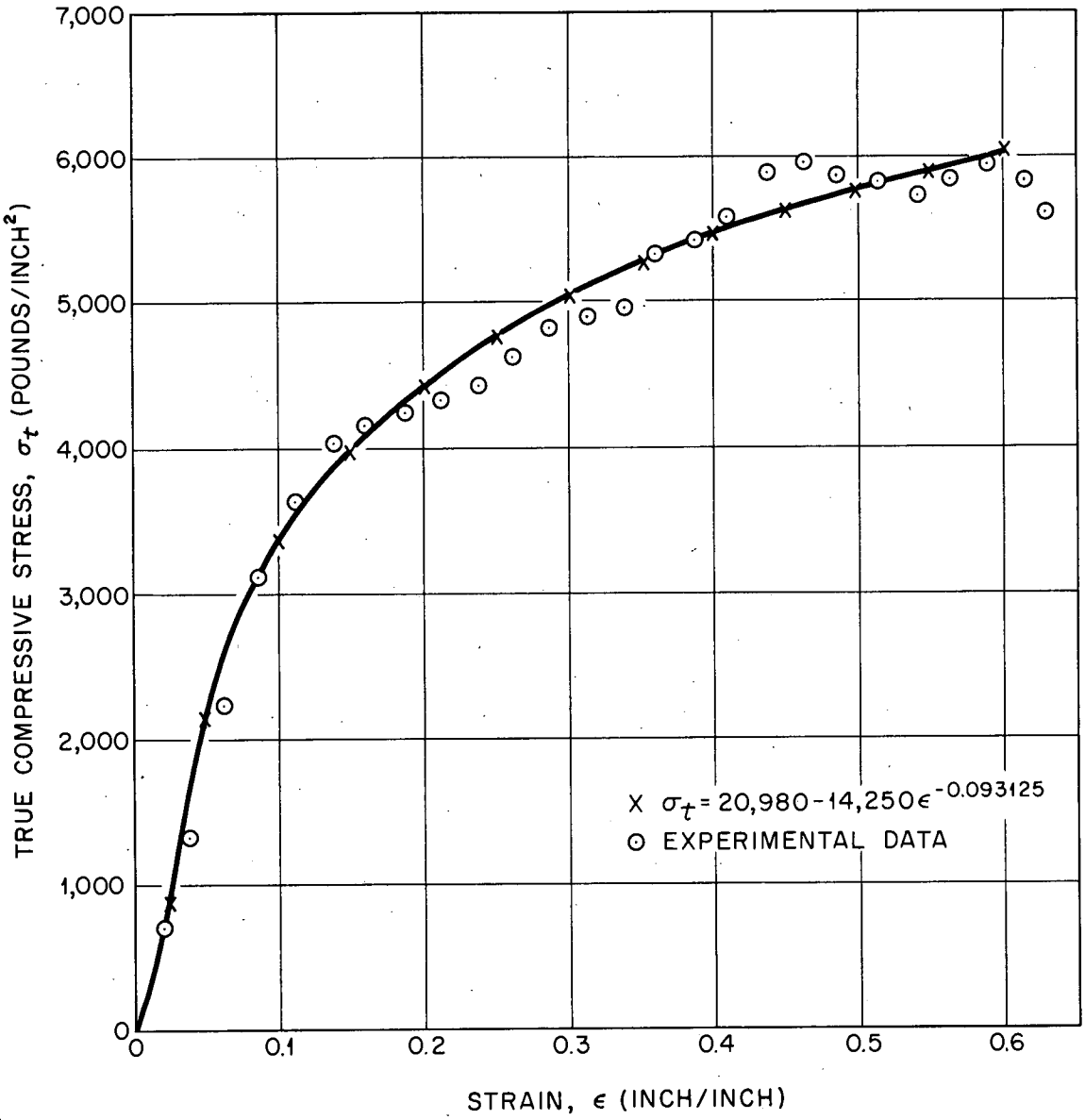

Figure 5.7. Plot of Equation 5.31 Compared With Plot of Experimental Data.

Similarly, the equation

$$\sigma_e = \frac{20,980 - 14,250\epsilon^{-0.093}}{(1 - \epsilon)} \tag{5.32}$$

describes the dynamic engineering stress-strain curve for lead. The curves for the true stress and the dynamic engineering stress as a function of engineering strain are illustrated in Figure 5.8.

The use of Equation 5.32 in some calculations will require difficult mathematical manipulations. When this is the case and a lower level of computational accuracy can be tolerated, an approximate straight-line equation having the general form

$$\sigma_e = m\epsilon + b \tag{5.33}$$

may be used in lieu of Equation 5.32. The constants m, which is the slope of the straight line, and b, which is the σ_e intercept, in Equation 5.33 were evaluated for the straight line illustrated in Figure 5.8 to develop the equation

$$\sigma_e = 16,680\epsilon + 2,050 \ . \tag{5.34}$$

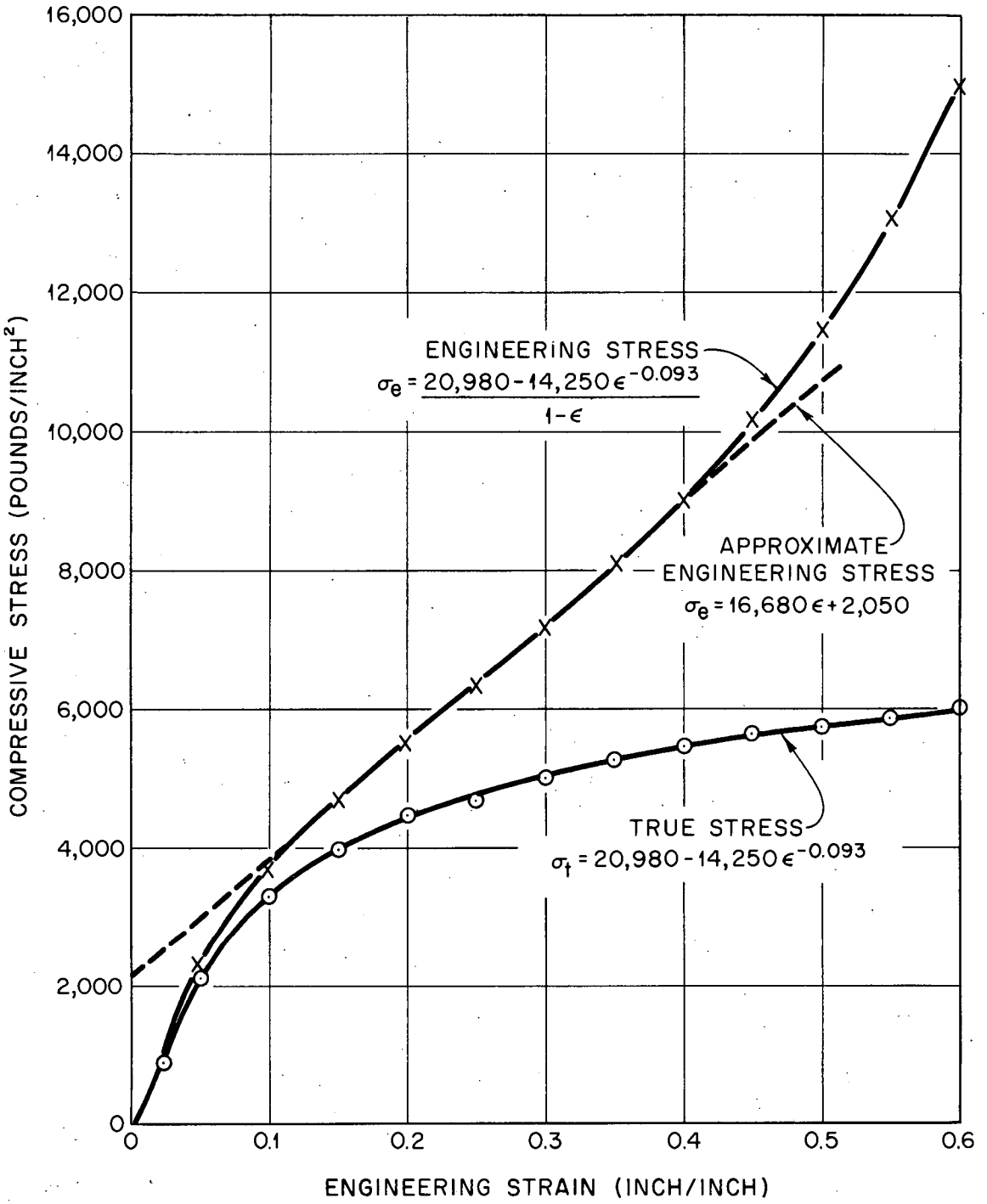

Figure 5.8. Curves of True Stress and Dynamic Engineering Stress as a Function of Engineering Strain Plotted from Equations Derived from Impact Test Data.

6. SUMMARY, CONCLUSIONS, AND RECOMMENDATIONS

6.1 Summary

To summarize before drawing conclusions and making recommendations, 68 specimens were impact tested to determine dynamic stress-strain data for chemical lead conforming to American Society for Testing and Materials Specification B29. Force was measured and recorded as a function of time by using a load cell, oscilloscope, and photography equipment. The force-time data were converted to acceleration-time data and numerically integrated, and the IBM 360 computer was used to obtain velocity as a function of time. A second integration yielded displacement as a function of time. After converting force to stress and true stress and converting displacement to strain, true stress-strain curves were plotted. The equation

$$\sigma_t = 20{,}980 - 14{,}250\epsilon^{-0.093} \tag{5.31}$$

was written by using those data which indicated that at least 95% of the available kinetic energy had been recorded. Equation 5.31 adequately represents the experimental impact test data up to a strain of 0.50 inch per inch. Beyond this value of strain, the small number of data points makes the experimental data somewhat suspect.

Reasonable agreement between the empirical Equation 5.31 and Equation 2.8 reported by Mok and Duffy (6) is illustrated in Figure 6.1. The lack of agreement between Equation 5.31 and Equation 2.9 derived by Slater, Johnson, and Aku (8) is also illustrated in Figure 6.1. This lack of agreement is not totally unexpected since the constants in

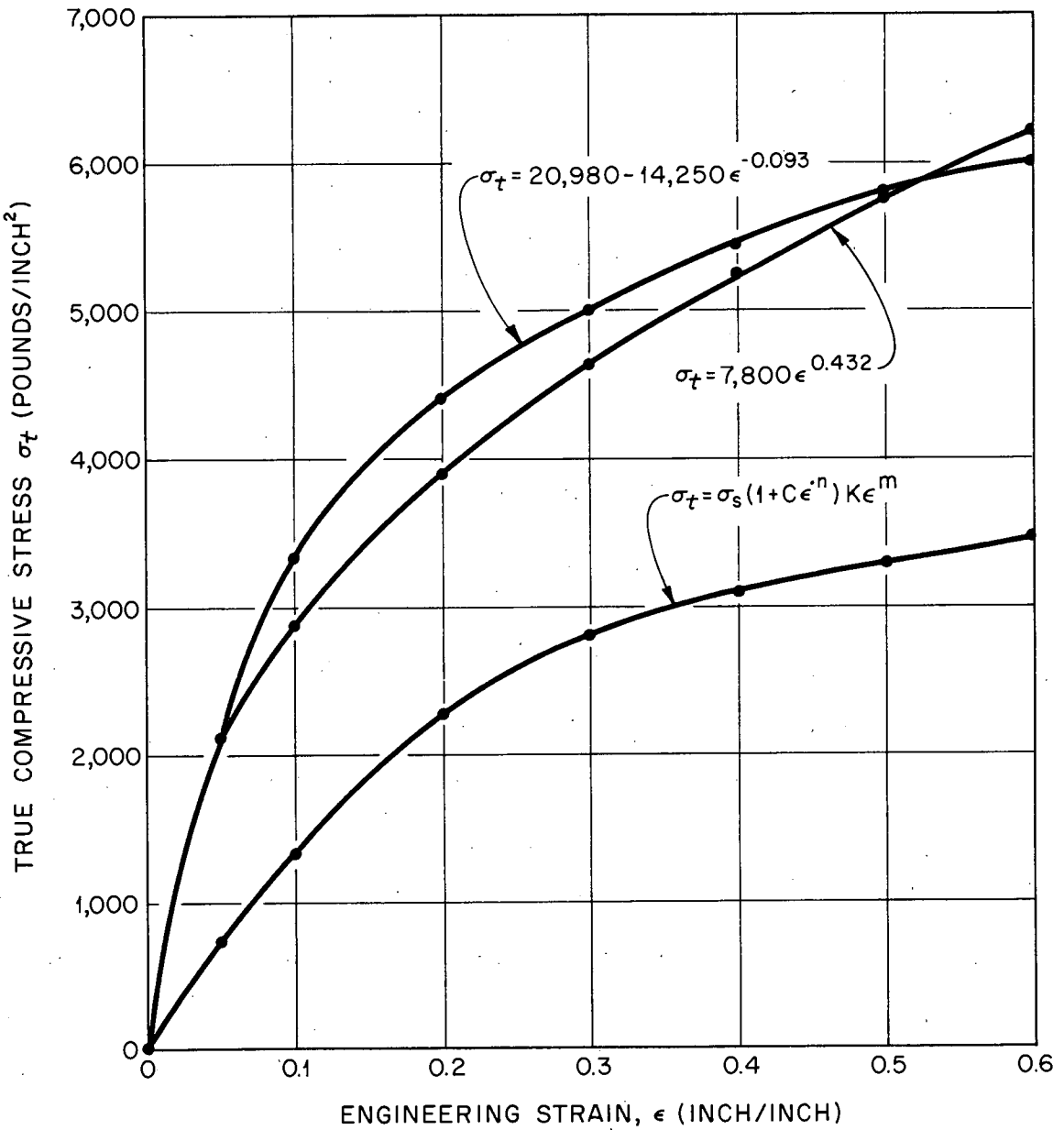

Figure 6.1. Comparison of Plots of Empirical Equation 5.31, Equation 2.8, and Equation 2.9.

Equation 2.9 that are equivalent to b, k, and m in Equation 5.31 were determined at significantly lower strain rates and somewhat lower strains than given by the data from which Equation 5.31 was developed. Another factor entering into this lack of agreement is that the properties of the "pure" lead used by Slater, Johnson, and Aku (8) and those of chemical lead may differ to some extent.

A comparison of curves plotted from experimental dynamic test data with curves plotted from static test data on stress-strain properties of lead very clearly demonstrates that the use of static data for design calculations would result in an ultraconservative design.

6.2 Conclusions

The single objective of this experimental investigation was to establish a usable stress-strain relationship for chemical lead conforming to the American Society for Testing and Materials Specification B29 for gross deflections at or near the strain rates experienced in the 30-foot free-fall condition of the hypothetical accident specified in the Code of Federal Regulations (1). With regard to this objective, four general conclusions may be drawn.

1. Equation 5.31 developed empirically adequately represents the dynamic stress-strain relationship for chemical lead within the limits of the impact test data. It is felt that this relationship can be applied to real design problems with approximately the same accuracy as is normally encountered when published material property data are used.

2. Chemical lead is not significantly strain-rate sensitive in the range of the strain rates encountered in the specified 30-foot free-fall accident condition.

3. The experimental techniques utilized in the impact tests performed in this investigation afford an economical method of developing stress-strain or force-deflection data for lead.

4. It is further concluded that the experimental techniques used in this investigation can be successfully employed to determine stress-strain relationships for other ductile materials. However, it is recognized that determination of stress-strain relationships for materials such as steel, stainless steel, and even aluminum will entail some difficulties not encountered with lead. These difficulties may include significant rebound of the impacting weight, a secondary impact, reflected stress waves, and probably a shorter time duration for the impact incident. A hardened alloy steel weight and load cell would be required.

6.3 Recommendations

In view of the lack of dependence of stress-strain properties of lead on strain rate, it is recommended that the equation for true stress

$$\sigma_t = 20{,}980 - 14{,}250\epsilon^{-0.093} , \tag{5.31}$$

the equation for engineering stress

$$\sigma_e = \frac{(20{,}980 - 14{,}250\epsilon^{-0.093})}{(1 - \epsilon)} \tag{5.32}$$

developed by using Equation 5.31 and the relationship given by Equation 5.30, and the curves plotted from these equations illustrated in Figure 5.8 (page 51) be used to compute the deflections and

accelerations of lead shielding in shipping casks which are being evaluated to determine their compliance with the regulations (1) governing the 30-foot free-fall accident condition. When a lower level of accuracy can be tolerated, the approximate Equation 5.34 may be used.

To further assure the adequacy of Equation 5.31 and verify the various analytical treatments of the impact condition, it is recommended that another series of impact tests be conducted. In these tests, lead cylinders should be dropped on a load cell and the force measured with respect to time. The lead cylinders dropped should have circumferential scribe marks at appropriate intervals so that the final deformation of each cylinder with respect to position along its length can be determined. This information can be used to determine the adequacy of Equation 5.31.

It is also recommended that the experimental techniques utilized in the impact tests performed in this investigation be used to determine the dynamic stress-strain characteristics under the specified 30-foot free-fall accident condition of the cladding materials commonly used on shipping casks for radioactive materials. These are ASTM Grade A-516 steel and AISC Type 304L stainless steel.

Finally, it is recommended that scale models of lead-filled shipping casks complete with cladding be dropped in a fully instrumented series of impact tests to develop and/or verify an adequate engineering model which could be used to calculate the effects of the 30-foot free-fall impact in future evaluations of shipping casks for radioactive materials.

LIST OF REFERENCES

1. Code of Federal Regulations, Title 10, Part 71, Transport of Licensed Materials; also see Federal Register, Vol. 31, pp. 9941-9949, July 1966.

2. D. Tabor, pp. 120-138 in The Hardness of Metals, Oxford University Press, London, 1951.

3. J. H. Vincent, "Experiments on Impact," Proceedings of the Cambridge Philosophical Society, Vol. 10, p. 332, 1898-1900.

4. A. W. Crook, "A Study of Some Impacts Between Metal Bodies By a Piezo Electric Method," Proceedings of the Royal Society, Vol. A212, p. 377, 1952.

5. C. H. Mok and J. Duffy, "The Behavior of Metals at Elevated Temperatures Under Impact With a Bouncing Ball," International Journal of Mechanical Science, Pergamon Press Ltd., Oxford, Vol. 6, pp. 161-175, 1963.

6. C. H. Mok and J. Duffy, "The Dynamic Stress-Strain Relation of Metals As Determined From Impact Tests With a Hard Ball," International Journal of Mechanical Science, Pergamon Press Ltd., Oxford, Vol. 7, pp. 355-371, 1964.

7. J. M. Gondusky and J. Duffy, "The Dynamic Stress-Strain Relationship of Lead and Its Dependence on Grain Structure," Technical Report Number 53, Division of Engineering, Brown University, Providence, Rhode Island, May 1967.

8. R. A. C. Slater, W. Johnson, and S. Y. Aku, "Experiments in the Fast Upsetting of Short Pure Lead Cylinders and a Tentative Analysis," International Journal of Mechanical Science, Pergamon Press Ltd., Oxford, Vol. 10, pp. 169-186, 1968.

9. "Course Notes" for Engineering Graphics 310, Department of Engineering Graphics, University of Cincinnati, Cincinnati, Ohio, pp. 1-8.

APPENDIXES

APPENDIX A

DATA TRANSFORMATION COMPUTER PROGRAM

A Fortran program applicable to the IBM 360 computer was written to transform the force-time data recorded during the impact tests of 68 specimens of chemical lead into stress-strain data. This program, which is discussed in Section 5.1 of this document, is presented on the following pages.

```
**FTN,L,M,E,G,A.
C THIS PROGRAM TRANSFORMS FORCE-TIME DATA INTO STRESS-STRAIN RELATIONS
C FOR RIGHT CIRCULAR CYLINDERS IMPACTED BY A FREE FALLING BODY
C CODED BY JOHN EVANS OAK RIDGE NATIONAL LAB OCTOBER 1969
C                    GLOSSARY OF NOTATION
C                    I=SPCIMEN IDENTIFICATION NUMBER
C                    J=DATA POINT IDENTIFICATION NUMBER
C                    NN= NUMBER OF DATA POINTS PER SPECIMEN
C                    F=FORCE IN POUNDS
C                    A=ACCELERATION IN FEET/SEC./SEC.
C                    H=ELEVATION IN INCHES
C                    W=WEIGHT OF THE IMPACTING HAMMER IN POUNDS
C                    D=SPCIMEN DIA. IN INCHES
C                    C=SPECIMEN INITIAL LENGTH IN INCHES
C                    B=SPECIMEN FINAL (DEFORMED) LENGTH IN INCHES
C                    V=VELOCITY IN FEET/SEC.
C                    VO= VELOCITY OF THE HAMMER AND SPECIMEN AT
C                        T=0 IN FEET/SEC.
C                    S=ENGINEERING STRESS IN POUNDS/SQ.INCH
C                    ST=TRUE STRESS IN POUNDS/SQ.INCH
C                    X=SPECIMEN DEFORMATION IN INCHES
C                    T=TIME IN SECONDS
C                    XE=STRAIN IN INCHES/INCH
C                    XA=SPECIMEN ACTUAL (MEASURED) FINAL DEFORMATION
C                    XEDOT=STRAIN RATE IN INCHES/INCH/SEC
C                    PED=PERCENTAGE ENERGY ACCOUNTED FOR
C                    PXD=PERCENTAGE DEFORMATION ACCOUNTED FOR
C                    AXEDOT=AVERAGE STRAIN RATE
      DIMENSION F(68,25),A(68,25),H(68),W(68),D(68),C(68),B(68),V(68,25)
     1,S(68,25),NN(68),VO(68),X(68,25),XE(68,25),ST(68,25),XA(68)
     2,PED(68),XEDOT(68,25),AXEDOT(68),PXD(68),T(68,25)
 1001 FORMAT(I2,F8.1,6F10.1/(7F10.1))
 1002 FORMAT(7F10.3/(7F10.3))
 1003 FORMAT(7F10.2/(7F10.2))
 1004 FORMAT(7F10.1/(7F10.1))
```

```
C ZERO STORAGE REGISTERS FOR ALL SUBSCRIPTED VARIABLES
      DO 1 I=1,68
      H(I)=0.0
      W(I)=0.0
      D(I)=0.0
      C(I)=0.0
      B(I)=0.0
      NN(I)=0
      VO(I)=0.0
      PFD(I)= 0.0
      AXEDOT(I)=0.0
      PXD(I)=0.0
 1    XA(I)=0.0
      DO 2 I=1,68
      DO 2 J=1,25
      F(I,J)=0.0
      A(I,J)=0.0
      V(I,J)=0.0
      S(I,J)=0.0
      X(I,J)=0.0
      XE(I,J)=0.0
      XEDOT(I,J)=0.0
      T(I,J)=0.0
 2    ST(I,J)=0.0
C READ IN TEST DATA
      DO 3  I =1,68
      READ 1001, N,(F(I,J), J= 1,N)
 3    NN(I) = N
      READ 1002, (D(I),I=1,68)
      READ 1002, (C(I),I=1,68)
      READ 1002, (B(I),I=1,68)
      READ 1003, (W(I),I=1,68)
      READ 1004, (H(I),I=1,68)
C CONVERT FORCE-TIME TO ACCELERATION-TIME BY NEWTON SECOND LAW
      DO 5  I= 1,68
      DO 4  J = 1,NN(I)
```

```
 4     A(I,J)=(F(I,J)*32.0)/(W(I)-(D(I)*D(I)*C(I)*0.161))
 5     CONTINUE
C COMPUTE VELOCITY AT T=0
       DO 6  I = 1,68
 6     VO(I)=SQRT(64.0*H(I)/12.0)/(1.0+(D(I)*D(I)*C(I)*0.161)/W(I))
C COMPUTE VELOCITY BY INTEGRATING THE ACCERATION-TIME CURVE BY SIMPSONS
C TIME INCREMENT IS CONSTANT AT .0001 SEC.
C J IS ODD
       DO 9  I = 1,68
 7     EO = 0.0
       EE = 0.0
       DO 8 J=3,NN(I),2
       EO = EO + A(I,J-2)
       EE = EE +A(I,J-1)
 8     V(I,J)=VO(I)-(0.0001/3.0)*(A(I,J)-A(I,1)+4.0*EE+2.0*EO)
      1  -0.0001*A(I,1)/2.0
 9     CONTINUE
C J IS EVEN
       DO 12 I =1,68
 10    EO =0.0
       EE =0.0
       DO 11 J = 2,NN(I),2
       EO = EO + A(I,J-1)
       IF (J.EQ.2) GO TO 11
       EE = EE + A(I,J-2)
 11    V(I,J)=VO(I)-(0.0001/3.0)*(A(I,J)+4.0*EO+2.0*EE)
 12    CONTINUE
C J IS ONE
       DO 13 I = 1,68
 13    V(I,1)=VO(I)-A(I,1)*0.0001/2.0
C COMPUTE SPECIMEN DEFORMATION BY INTEGRATING THE VELOCITY-TIME CURVE BY
C SIMPSONS RULE - TIME INCREMENT IS CONSTANT AT .0001 SEC.
C J IS ODD
       DO 16 I = 1,68
 14    EO = 0.0
       EE = 0.0
```

```
      DO 15 J = 3,NN(I),2
      EO = EO + V(I,J-2)
      EE =EE + V(I,J-1)
 15   X(I,J)=0.0004*(V(I,J)-V(I,1)+4.0*EE+2.0*EO)+0.0006*(VO(I)+V(I,1))
 16   CONTINUE
C J IS EVEN
      DO 19 I = 1,68
 17   EO = 0.0
      EE = 0.0
      DO 18 J= 2,NN(I),2
      EO = EO + V(I,J-1)
      IF (J.EQ.2) GO TO 18
      EE=EE+V(I,J-2)
 18   X(I,J)=0.0004*(VO(I)+V(I,J)+4.0*EO+2.0*EE)
 19   CONTINUE
C J IS ONE
      DO 20 I= 1,68
 20   X(I,1)=(VO(I)+V(I,1))*0.0006
C COMPUTE STRAIN
      DO 22 I=1,68
      DO 21 J=1,NN(I)
 21   XE(I,J)=X(I,J)/C(I)
 22   CONTINUE
C COMPUTE ENGINEERING STRESS
      DO 24 I=1,68
      DO 23 J=1,NN(I)
 23   S(I,J)=(1.273*F(I,J))/(D(I)*D(I))
 24   CONTINUE
C COMPUTE TRUE STRESS
      DO 26 I=1,68
      DO 25 J=1,NN(I)
 25   ST(I,J)=F(I,J)*(1.0-XE(I,J))*1.273/(D(I)*D(I))
 26   CONTINUE
C COMPUTE ACTUAL FINAL DEFORMATION
      DO 27 I=1,68
```

```
 27    XA(I)=C(I)-B(I)
       DO 28 I=1,68
       DO 28 J=1,NN(I)
 28    WRITE(51,1005)I,J,D(I),C(I),H(I),W(I),V(I,J),X(I,J),XA(I),XE(I,J),
      1   S(I,J),ST(I,J),A(I,J),F(I,J),VO(I)
 1005  FORMAT (2I4,2X,F6.3,2X,F6.3,2X,F6.1,2X,F6.3,2X,F6.2,2X,F6.3,2X,
      1  F6.3,2X,F6.3,2X,F8.1,2X,F8.1,2X,F9.2,2X,F8.1,2X,F6.2,2X,F8.3)
C GROUP TRUE STRESS AND STRAIN BY INCREMENTS OF 0.025-AVERAGE STRESS
C AND STRAIN OVER THE INCREMENT-COMPUTE THE STANDARD DEVIATION OF STRESS
C AND STRAIN
 1006  FORMAT(3X,I2,3X,I2,3X,F8.1,3X,F6.3)
       DO 33 K=1,28
       INDEX = 0
       SUMST = 0.0
       SUM2ST = 0.0
       SUMXE = 0.0
       SUM2XE = 0.0
       G=(K-1)*0.025
       E=K*0.025
       DO 30 I=1,68
       DO 29 J=1,NN(I)
       IF((XE(I,J).LT.E).AND.(XE(I,J).GE.G)) WRITE(51,1006) I,J,
      1 ST(I,J),XE(I,J)
       IF((XE(I,J).GE.E) .OR. (XE(I,J) .LT.G)) GO TO 29
C GROUP ST AND XE BY XE INCREMENTS OF 0.025 - AVERAGE ST AND XE OVER
C THE INCREMENT - COMPUTE THE STANDARD DEVIATION OF ST AND XE
       INDEX = INDEX + 1
       SUMST = SUMST + ST(I,J)
       SUM2ST = SUM2ST + ST(I,J)*ST(I,J)
       SUMXE = SUMXE + XE(I,J)
       SUM2XE = SUM2XE + XE(I,J)*XE(I,J)
 29    CONTINUE
 30    CONTINUE
       IF(INDEX.EQ.0) GO TO 32
       IF(INDEX.EQ.1) SDST = 0.0
       IF(INDEX.EQ.1) SDXE = 0.0
```

```
      IF(INDEX.EQ.1) GO TO 31
      SDST =SQRT((1./(INDEX-1))*(SUM2ST - SUMST*SUMST/INDEX))
      SDXE =SQRT((1./(INDEX-1))*(SUM2XE - SUMXE*SUMXE/INDEX))
 31   STAVG= SUMST/INDEX
      XEAVG = SUMXE/INDEX
      WRITE(51,1007) STAVG,XEAVG,SDST,SDXE
 1007 FORMAT(36X,F10.1,2X,F10.3,2X,F10.3,2X,F10.4)
 32   CONTINUE
 33   CONTINUE
C ELIMINATE DATA WHICH DOES NOT ACCOUNT FOR AT LEAST 90.0 PERCENT OF THE
      DO 39 K=1,28
      INDEX = 0
      SUMST = 0.0
      SUM2ST = 0.0
      SUMXE = 0.0
      SUM2XE = 0.0
      G=(K-1)*0.025
      E=K*0.025
      DO 36 I=1,68
      L=NN(I)
      PED(I)=(1.0-V(I,L)*V(I,L)*12.0/(64.0*H(I)))*100.0
      IF(PED(I).LT.90.0) GO TO 35
      DO 34 J=1,NN(I)
      IF((XE(I,J).LT.E).AND.(XE(I,J).GE.G)) WRITE(51,1006) I,J,
     1 ST(I,J),XE(I,J)
      IF((XE(I,J).GE.E) .OR. (XE(I,J) .LT.G)) GO TO 34
C GROUP ST AND XE BY XE INCREMENTS OF 0.025 - AVERAGE ST AND XE OVER
C THE INCREMENT - COMPUTE THE STANDARD DEVIATION OF ST AND XE
      INDEX = INDEX + 1
      SUMST = SUMST + ST(I,J)
      SUM2ST = SUM2ST + ST(I,J)*ST(I,J)
      SUMXE = SUMXE + XE(I,J)
      SUM2XE = SUM2XE + XE(I,J)*XE(I,J)
 34   CONTINUE
 35   CONTINUE
```

```
 36   CONTINUE
      IF(INDEX.EQ.0) GO TO 38
      IF(INDEX.EQ.1) SDXE = 0.0
      IF(INDEX.EQ.1) SDST = 0.0
      IF(INDEX.EQ.1) GO TO 37
      SDST =SQRT((1./(INDEX-1))*(SUM2ST - SUMST*SUMST/INDEX))
      SDXE =SQRT((1./(INDEX-1))*(SUM2XE - SUMXE*SUMXE/INDEX))
 37   STAVG= SUMST/INDEX
      XEAVG = SUMXE/INDEX
      WRITE(51,1007) STAVG,XEAVG,SDST,SDXE
 38   CONTINUE
 39   CONTINUE
C ELIMINATE DATA WHICH DOES NOT ACCOUNT FOR AT LEAST 95.0 PERCENT OF THE
      DO 45 K=1,28
      INDEX = 0
      SUMST = 0.0
      SUM2ST = 0.0
      SUMXE = 0.0
      SUM2XE = 0.0
      G=(K-1)*0.025
      E=K*0.025
      DO 42 I=1,68
      L=NN(I)
      IF(PED(I).LT.95.0) GO TO 41
      DO 40 J=1,NN(I)
      IF((XE(I,J).LT.E).AND.(XE(I,J).GE.G)) WRITE(51,1006) I,J,
     1 ST(I,J),XE(I,J)
      IF((XE(I,J).GE.E) .OR. (XE(I,J) .LT.G)) GO TO 40
C GROUP ST AND XE BY XE INCREMENTS OF 0.025 - AVERAGE ST AND XE OVER
C THE INCREMENT - COMPUTE THE STANDARD DEVIATION OF ST AND XE
      INDEX = INDEX + 1
      SUMST = SUMST + ST(I,J)
      SUM2ST = SUM2ST + ST(I,J)*ST(I,J)
      SUMXE = SUMXE + XE(I,J)
      SUM2XE = SUM2XE + XE(I,J)*XE(I,J)
 40   CONTINUE
```

```
 41    CONTINUE
 42    CONTINUE
       IF(INDEX.EQ.0) GO TO 44
       IF(INDEX.EQ.1) SDXE = 0.0
       IF(INDEX.EQ.1) SDST = 0.0
       IF(INDEX.EQ.1) GO TO 43
       SDST =SQRT((1./(INDEX-1))*(SUM2ST - SUMST*SUMST/INDEX))
       SDXE =SQRT((1./(INDEX-1))*(SUM2XE - SUMXE*SUMXE/INDEX))
 43    STAVG= SUMST/INDEX
       XEAVG = SUMXE/INDEX
       WRITE(51,1007) STAVG,XEAVG,SDST,SDXE
 44    CONTINUE
 45    CONTINUE
C COMPUTE STRAIN RATE
       DO 47 I=1,68
       DO 46 J=1,NN(I)
 46    XEDOT(I,J)=(V(I,J)*12.)/(C(I)-X(I,J))
 47    CONTINUE
C GROUP DATA FOR STRAIN RATE BY INCREMENTS OF 20.0 INCHES/INCH/SEC
       DO 49 K=1,45
       G=(K-1)*20.0
       E=K*20.0
       DO 48 I=1,68
       DO 48 J=1,NN(I)
 48    IF((XEDOT(I,J).LT.E).AND.(XEDOT(I,J).GE.G)) WRITE(51,1008)I,J,
      1 XEDOT(I,J),ST(I,J),XE(I,J)
 1008  FORMAT (3X,I2,3X,I2,3X,F8.3,3X,F8.1,3X,F6.3)
 49    CONTINUE
C COMPUTE AVERAGE STRAIN RATE
       DO 50 I=1,68
 50    AXEDOT(I)=VO(I)*6.0/C(I)
       DO 57 KK=1,6
       GG=9.0+55.0*KK
       EE=64.0+55.0*KK
       DO 56 K=1,28
       INDEX = 0
```

```
      SUMST = 0.0
      SUM2ST = 0.0
      SUMXE = 0.0
      SUM2XE = 0.0
      G=(K-1)*0.025
      E=K*0.025
      DO 53 I=1,68
      DO 52 J=1,NN(I)
      IF((XE(I,J).LT.E).AND.(XE(I,J).GE.G).AND.(AXEDOT(I).LT.EE).AND.
     1AXEDOT(I).GE.GG) WRITE(51,1009) AXEDOT(I),ST(I,J),XE(I,J)
 1009 FORMAT(2X,F9.2,2X,F10.1,2X,F7.3)
      IF((XE(I,J).GE.E) .OR. (XE(I,J) .LT.G)) GO TO 52
      IF((AXEDOT(I).GE.EE).OR.(AXEDOT(I).LT.GG)) GO TO 51
C GROUP ST AND XE BY XE INCREMENTS OF 0.025 - AVERAGE ST AND XE OVER
C THE INCREMENT - COMPUTE THE STANDARD DEVIATION OF ST AND XE
      INDEX = INDEX + 1
      SUMST = SUMST + ST(I,J)
      SUM2ST = SUM2ST + ST(I,J)*ST(I,J)
      SUMXE = SUMXE + XE(I,J)
      SUM2XE = SUM2XE + XE(I,J)*XE(I,J)
 51   CONTINUE
 52   CONTINUE
 53   CONTINUE
      IF(INDEX.EQ.0) GO TO 55
      IF(INDEX.EQ.1) SDST = 0.0
      IF(INDEX.EQ.1) SDXE = 0.0
      IF(INDEX.EQ.1) GO TO 54
      SDST =SQRT((1./(INDEX-1))*(SUM2ST - SUMST*SUMST/INDEX))
      SDXE =SQRT((1./(INDEX-1))*(SUM2XE - SUMXE*SUMXE/INDEX))
 54   STAVG= SUMST/INDEX
      XEAVG = SUMXE/INDEX
      WRITE(51,1010) STAVG,XEAVG,SDST,SDXE
 1010 FORMAT(36X,F10.1,2X,F10.3,2X,F10.3,2X,F10.4)
 55   CONTINUE
 56   CONTINUE
```

```
57    CONTINUE
      DO 59 I=1,68
      L=NN(I)
58    PXD(I)=((XA(I)-X(I,L))/XA(I))*100.0
59    CONTINUE
      DO 61 I=1,68
      DO 60 J=1,NN(I)
60    T(I,J)= J*0.0001
61    CONTINUE
      DO 67 I =1,65,4
      I1=I+1
      I2=I+2
      I3=I+3
      WRITE(51,1011)  I ,I1 , I2 , I3
1011  FORMAT (21H1    SPECIMEN NUMBER ,I2,3X,16HSPECIMEN NUMBER ,
     1        I2,3X,16HSPECIMEN NUMBER ,I2,3X,16HSPECIMEN NUMBER,I2)
      WRITE(51,1012)
1012  FORMAT (1H0)
      WRITE(51,1013)
1013  FORMAT ( 1H ,7X,4HTIME,5X,5HFORCE,7X,4HTIME,5X,5HFORCE,7X,4HTIME,
     1        5X,5HFORCE,7X,4HTIME,5X,5HFORCE)
      WRITE(51,1014)
1014  FORMAT (1H ,8X,2HIN,8X,2HIN,9X,2HIN,8X,2HIN,9X,2HIN,8X,2HIN,9X,
     1        2HIN,8X,2HIN)
      WRITE(51,1015)
1015  FORMAT (1H ,4X,7HSECONDS,4X,6HPOUNDS,4X,7HSECONDS,4X,6HPOUNDS,4X,
     1        7HSECONDS,4X,6HPOUNDS,4X,7HSECONDS,4X,6HPOUNDS)
      WRITE(51,1012)
      DO 66 J =1,25
      WRITE(51,1016)
1016  FORMAT(1H ,1X)
      DO 65 K =1,4
      IF (T(I+K-1,J).EQ.0.0) GO TO 65
      IF(K.NE.1) GO TO 62
      WRITE(51,1017) T(I+K-1,J), F(I+K-1,J)
```

```
1017 FORMAT(1H+, 3X,F8.4,3X,F7.1)
     GO TO 65
62   IF(K.NE.2) GO TO 63
     WRITE(51,1018) T(I+K-1,J), F(I+K-1,J)
1018 FORMAT(1H+,24X,F8.4,3X,F7.1)
     GO TO 65
63   IF(K.NE.3) GO TO 64
     WRITE(51,1019) T(I+K-1,J), F(I+K-1,J)
1019 FORMAT(1H+,45X,F8.4,3X,F7.1)
     GO TO 65
64   WRITE(51,1020) T(I+K-1,J), F(I+K-1,J)
1020 FORMAT(1H+,66X,F8.4,3X,F7.1)
65   CONTINUE
66   CONTINUE
67   CONTINUE
     WRITE(51,1021)
1021 FORMAT ( 1H1, 1HI,5X,1HD,7X,1HC,7X,1HB,7X,1HH,7X,1HW,6X,2HVO,6X,
    1         2HXA,4X,6HAXEDOT,3X,3HPED,4X,3HPXD)
     WRITE(51,1022)
1022 FORMAT(1H )
     DO 68 I=1,34
68   WRITE(51,1023) I,D(I),C(I),B(I),H(I),W(I),VO(I),XA(I),AXEDOT(I),
    1               PED(I),PXD(I)
1023 FORMAT (X,I2,3X,F5.3,3X,F5.3,3X,F5.3,3X,F5.1,3X,F5.2,3X,F4.1,3X,
    1         F5.3,3X,F5.1,3X,F4.1,3X,F5.1)
     WRITE(51,1021)
     DO 69 I=35,68
69   WRITE(51,1023) I,D(I),C(I),B(I),H(I),W(I),VO(I),XA(I),AXEDOT(I),
    1               PED(I),PXD(I)
     CALL EXIT
     STOP
     END
```

SPECIMEN NUMBER 1		SPECIMEN NUMBER 2		SPECIMEN NUMBER 3		SPECIMEN NUMBER 4	
TIME IN SECONDS	FORCE IN POUNDS	TIME IN SECONDS	FORCE IN POUNDS	TIME IN SECONDS	FORCE IN POUNDS	TIME IN SECONDS	FORCE IN POUNDS
0.0001	1250.0	0.0001	832.0	0.0001	624.0	0.0001	832.0
0.0002	2500.0	0.0002	1664.0	0.0002	1456.0	0.0002	1788.0
0.0003	3437.5	0.0003	2496.0	0.0003	2496.0	0.0003	2787.2
0.0004	4062.5	0.0004	3328.0	0.0004	2912.0	0.0004	3411.2
0.0005	4375.0	0.0005	3952.0	0.0005	3536.0	0.0005	3827.2
0.0006	4687.5	0.0006	4160.0	0.0006	3952.0	0.0006	4160.0
0.0007	5312.5	0.0007	4576.0	0.0007	4368.0	0.0007	4576.0
0.0008	5625.0	0.0008	4992.0	0.0008	4784.0	0.0008	5200.0
0.0009	6250.0	0.0009	5824.0	0.0009	5408.0	0.0009	5782.4
0.0010	6875.0	0.0010	6240.0	0.0010	6032.0	0.0010	6198.4
0.0011	7187.5	0.0011	6656.0	0.0011	6364.8	0.0011	6531.2
0.0012	7500.0	0.0012	7072.0	0.0012	6656.0	0.0012	6780.8
0.0013	7500.0	0.0013	7280.0	0.0013	6780.8	0.0013	6988.8
		0.0014	7280.5	0.0014	6864.0	0.0014	6988.8

SPECIMEN NUMBER 5		SPECIMEN NUMBER 6		SPECIMEN NUMBER 7		SPECIMEN NUMBER 8	
TIME IN SECONDS	FORCE IN POUNDS	TIME IN SECONDS	FORCE IN POUNDS	TIME IN SECONDS	FORCE IN POUNDS	TIME IN SECONDS	FORCE IN POUNDS
0.0001	540.0	0.0001	499.2	0.0001	624.0	0.0001	707.0
0.0002	1456.0	0.0002	1456.0	0.0002	1664.0	0.0002	1664.0
0.0003	2288.0	0.0003	2288.0	0.0003	2579.2	0.0003	2912.0
0.0004	3203.2	0.0004	3030.8	0.0004	3411.2	0.0004	3660.8
0.0005	3744.0	0.0005	3328.0	0.0005	3868.8	0.0005	4076.8
0.0006	4160.0	0.0006	3619.2	0.0006	4201.6	0.0006	4284.8
0.0007	4576.0	0.0007	3868.8	0.0007	4576.0	0.0007	4659.2
0.0008	4992.0	0.0008	4409.6	0.0008	4992.0	0.0008	4992.0
0.0009	5491.0	0.0009	4908.8	0.0009	5408.0	0.0009	5408.0
0.0010	5907.2	0.0010	5408.0	0.0010	5824.0	0.0010	5907.2
0.0011	6489.6	0.0011	5616.0	0.0011	6198.4	0.0011	6364.8
0.0012	6867.0	0.0012	5782.4	0.0012	6364.8	0.0012	6531.2
0.0013	6988.8	0.0013	5865.6	0.0013	6489.6	0.0013	6656.0
0.0014	7072.0	0.0014	5907.2	0.0014	6572.8	0.0014	6656.0

SPECIMEN NUMBER 9		SPECIMEN NUMBER 10		SPECIMEN NUMBER 11		SPECIMEN NUMBER 12	
TIME IN SECONDS	FORCE IN POUNDS	TIME IN SECONDS	FORCE IN POUNDS	TIME IN SECONDS	FORCE IN POUNDS	TIME IN SECONDS	FORCE IN POUNDS
0.0001	416.0	0.0001	624.0	0.0001	540.8	0.0001	416.0
0.0002	1331.2	0.0002	1580.8	0.0002	1580.8	0.0002	1081.6
0.0003	2080.0	0.0003	2496.0	0.0003	2371.2	0.0003	1539.2
0.0004	2704.0	0.0004	3036.8	0.0004	2912.0	0.0004	1830.4
0.0005	3078.4	0.0005	3369.6	0.0005	3161.6	0.0005	2080.0
0.0006	3328.0	0.0006	3536.0	0.0006	3328.0	0.0006	2121.6
0.0007	3411.0	0.0007	3744.0	0.0007	3494.4	0.0007	2288.0
0.0008	3702.4	0.0008	4035.2	0.0008	3827.2	0.0008	2662.4
0.0009	4076.8	0.0009	4409.6	0.0009	4243.2	0.0009	3036.8
0.0010	4451.2	0.0010	4742.4	0.0010	4576.0	0.0010	3120.0
0.0011	4576.0	0.0011	4950.4	0.0011	4659.2	0.0011	3203.2
0.0012	4825.6	0.0012	5075.2	0.0012	4825.6	0.0012	3286.4
0.0013	4908.8	0.0013	5324.8	0.0013	4908.8	0.0013	3328.0
0.0014	4950.4	0.0014	5324.8	0.0014	4908.8	0.0014	3328.0
0.0015	4950.4						

SPECIMEN NUMBER 13		SPECIMEN NUMBER 14		SPECIMEN NUMBER 15		SPECIMEN NUMBER 16	
TIME IN SECONDS	FORCE IN POUNDS	TIME IN SECONDS	FORCE IN POUNDS	TIME IN SECONDS	FORCE IN POUNDS	TIME IN SECONDS	FORCE IN POUNDS
0.0001	540.8	0.0001	582.4	0.0001	416.0	0.0001	499.2
0.0002	1164.8	0.0002	1081.6	0.0002	1206.4	0.0002	1123.2
0.0003	1580.8	0.0003	1664.0	0.0003	1664.0	0.0003	1664.0
0.0004	1747.2	0.0004	1705.6	0.0004	1996.8	0.0004	1830.4
0.0005	2038.4	0.0005	1830.4	0.0005	2080.0	0.0005	1996.8
0.0006	2246.4	0.0006	1913.6	0.0006	2288.0	0.0006	2163.2
0.0007	2496.0	0.0007	2288.0	0.0007	2620.8	0.0007	2537.6
0.0008	2787.2	0.0008	2579.2	0.0008	3036.8	0.0008	2953.6
0.0009	2912.0	0.0009	2745.6	0.0009	3328.0	0.0009	3244.8
0.0010	3078.4	0.0010	2828.8	0.0010	3494.4	0.0010	3411.2
0.0011	3244.8	0.0011	3078.4	0.0011	3744.0	0.0011	3577.6
0.0012	3328.0	0.0012	3161.6	0.0012	3952.0	0.0012	3744.0
0.0013	3369.6	0.0013	3203.2	0.0013	4160.0	0.0013	4035.2
				0.0014	4409.6	0.0014	4201.6
				0.0015	4492.8	0.0015	4368.0
				0.0016	4659.2	0.0016	4451.2
				0.0017	4700.8	0.0017	4451.2
						0.0018	4451.2

SPECIMEN NUMBER 17		SPECIMEN NUMBER 18		SPECIMEN NUMBER 19		SPECIMEN NUMBER 20	
TIME IN SECONDS	FORCE IN POUNDS	TIME IN SECONDS	FORCE IN POUNDS	TIME IN SECONDS	FORCE IN POUNDS	TIME IN SECONDS	FORCE IN POUNDS
0.0001	624.0	0.0001	707.2	0.0001	499.2	0.0001	540.8
0.0002	1164.8	0.0002	1456.0	0.0002	1248.0	0.0002	956.8
0.0003	1580.8	0.0003	1664.0	0.0003	1955.2	0.0003	1372.8
0.0004	1872.0	0.0004	1747.2	0.0004	2246.4	0.0004	2038.4
0.0005	1955.2	0.0005	1996.8	0.0005	2579.2	0.0005	2496.0
0.0006	2412.8	0.0006	2412.8	0.0006	3036.8	0.0006	2828.8
0.0007	2662.4	0.0007	2870.4	0.0007	3577.6	0.0007	3244.8
0.0008	3036.8	0.0008	3078.4	0.0008	4160.0	0.0008	3577.6
0.0009	3203.2	0.0009	3328.0	0.0009	4534.4	0.0009	4035.2
0.0010	3411.2	0.0010	3536.0	0.0010	4950.4	0.0010	4576.0
0.0011	3660.8	0.0011	3785.6	0.0011	5283.2	0.0011	5033.6
0.0012	3952.0	0.0012	4035.2	0.0012	5699.2	0.0012	5408.0
0.0013	4160.0	0.0013	4160.0	0.0013	6115.2	0.0013	5824.0
0.0014	4284.8	0.0014	4368.0	0.0014	6281.6	0.0014	6115.2
0.0015	4368.0	0.0015	4451.2	0.0015	6656.0	0.0015	6364.8
0.0016	4409.6	0.0016	4492.8	0.0016	6739.2	0.0016	6656.0
0.0017	4431.2	0.0017	4534.4	0.0017	6864.0	0.0017	6780.8
				0.0018	6864.0	0.0018	6905.6
						0.0019	6905.6

SPECIMEN NUMBER 21		SPECIMEN NUMBER 22		SPECIMEN NUMBER 23		SPECIMEN NUMBER 24	
TIME IN SECONDS	FORCE IN POUNDS	TIME IN SECONDS	FORCE IN POUNDS	TIME IN SECONDS	FORCE IN POUNDS	TIME IN SECONDS	FORCE IN POUNDS
0.0001	499.2	0.0001	812.5	0.0001	750.0	0.0001	625.0
0.0002	1248.0	0.0002	1687.5	0.0002	1312.5	0.0002	1125.0
0.0003	1664.0	0.0003	2125.0	0.0003	2500.0	0.0003	1875.0
0.0004	2412.0	0.0004	2875.0	0.0004	3000.0	0.0004	2500.0
0.0005	2579.2	0.0005	3187.5	0.0005	3250.0	0.0005	2937.5
0.0006	2870.4	0.0006	3687.5	0.0006	3812.5	0.0006	3312.0
0.0007	3244.8	0.0007	4187.5	0.0007	4312.5	0.0007	3875.0
0.0008	3827.2	0.0008	4812.5	0.0008	5000.0	0.0008	4562.5
0.0009	4243.2	0.0009	5562.5	0.0009	5687.5	0.0009	5125.0
0.0010	4700.8	0.0010	6312.5	0.0010	6312.5	0.0010	5750.0
0.0011	5116.8	0.0011	6875.0	0.0011	7000.0	0.0011	6250.0
0.0012	5491.2	0.0012	7437.5	0.0012	7500.0	0.0012	6937.5
0.0013	5824.0	0.0013	8000.0	0.0013	7875.0	0.0013	7250.0
0.0014	6115.2	0.0014	8500.0	0.0014	8375.0	0.0014	7750.0
0.0015	6406.4	0.0015	9062.5	0.0015	8875.0	0.0015	8062.5
0.0016	6614.4	0.0016	9250.0	0.0016	9125.0	0.0016	8312.5
0.0017	6739.2	0.0017	9312.5	0.0017	9187.5	0.0017	8500.0
0.0018	6780.8					0.0018	8687.5
0.0019	6780.8						

SPECIMEN NUMBER 25		SPECIMEN NUMBER 26		SPECIMEN NUMBER 27		SPECIMEN NUMBER 28	
TIME IN SECONDS	FORCE IN POUNDS	TIME IN SECONDS	FORCE IN POUNDS	TIME IN SECONDS	FORCE IN POUNDS	TIME IN SECONDS	FORCE IN POUNDS
0.0001	1250.0	0.0001	812.5	0.0001	937.5	0.0001	1125.0
0.0002	1875.0	0.0002	1562.5	0.0002	1562.5	0.0002	1937.0
0.0003	2562.5	0.0003	2187.5	0.0003	2062.5	0.0003	2625.0
0.0004	3250.0	0.0004	2812.5	0.0004	2625.0	0.0004	3312.5
0.0005	3875.0	0.0005	3250.0	0.0005	3187.5	0.0005	3687.5
0.0006	4375.0	0.0006	3875.0	0.0006	3875.0	0.0006	4500.0
0.0007	5000.0	0.0007	4500.0	0.0007	4562.5	0.0007	5187.5
0.0008	5687.5	0.0008	5000.0	0.0008	5187.5	0.0008	6000.0
0.0009	6375.0	0.0009	5750.0	0.0009	5687.5	0.0009	6812.5
0.0010	7000.0	0.0010	6687.5	0.0010	6437.5	0.0010	7312.5
0.0011	7562.5	0.0011	7125.0	0.0011	7125.0	0.0011	8375.0
0.0012	8250.0	0.0012	7687.5	0.0012	7812.5	0.0012	8875.0
0.0013	8500.0	0.0013	8250.0	0.0013	8187.5	0.0013	9500.0
0.0014	8875.0	0.0014	8687.5	0.0014	8562.5	0.0014	9687.0
0.0015	9187.5	0.0015	9125.0	0.0015	8750.0	0.0015	10125.0
				0.0016	8875.0		

SPECIMEN NUMBER 29		SPECIMEN NUMBER 30		SPECIMEN NUMBER 31		SPECIMEN NUMBER 32	
TIME IN SECONDS	FORCE IN POUNDS	TIME IN SECONDS	FORCE IN POUNDS	TIME IN SECONDS	FORCE IN POUNDS	TIME IN SECONDS	FORCE IN POUNDS
0.0001	875.0	0.0001	750.0	0.0001	625.0	0.0001	750.0
0.0002	1687.5	0.0002	1437.5	0.0002	1500.0	0.0002	1876.0
0.0003	2500.0	0.0003	2250.0	0.0003	2312.5	0.0003	2375.0
0.0004	3187.5	0.0004	3062.5	0.0004	3062.5	0.0004	3125.0
0.0005	3875.0	0.0005	3687.5	0.0005	3562.5	0.0005	3500.0
0.0006	4375.0	0.0006	4375.0	0.0006	4125.0	0.0006	4187.0
0.0007	5125.0	0.0007	5000.0	0.0007	4687.5	0.0007	5000.0
0.0008	6062.5	0.0008	5687.5	0.0008	5562.5	0.0008	5750.0
0.0009	6875.0	0.0009	6562.5	0.0009	6187.5	0.0009	6375.0
0.0010	7625.0	0.0010	7437.5	0.0010	6875.0	0.0010	7125.0
0.0011	8500.0	0.0011	8312.5	0.0011	7437.5	0.0011	7625.0
0.0012	9250.0	0.0012	9187.5	0.0012	7812.5	0.0012	8125.0
0.0013	9875.0	0.0013	9875.0	0.0013	8187.5	0.0013	8437.5
0.0014	10250.0	0.0014	10312.5	0.0014	8562.5	0.0014	8500.0
0.0015	10500.0	0.0015	10625.0				

SPECIMEN NUMBER 33		SPECIMEN NUMBER 34		SPECIMEN NUMBER 35		SPECIMEN NUMBER 36	
TIME IN SECONDS	FORCE IN POUNDS	TIME IN SECONDS	FORCE IN POUNDS	TIME IN SECONDS	FORCE IN POUNDS	TIME IN SECONDS	FORCE IN POUNDS
0.0001	937.5	0.0001	1187.5	0.0001	937.5	0.0001	937.5
0.0002	1500.0	0.0002	2500.0	0.0002	2250.0	0.0002	1687.5
0.0003	2375.0	0.0003	3750.0	0.0003	3500.0	0.0003	2937.5
0.0004	3562.5	0.0004	4437.5	0.0004	4062.5	0.0004	4000.0
0.0005	3750.0	0.0005	4875.0	0.0005	4500.0	0.0005	4375.0
0.0006	4375.0	0.0006	5000.0	0.0006	4687.5	0.0006	4562.5
0.0007	5125.0	0.0007	5187.5	0.0007	4750.0	0.0007	4812.5
0.0008	5625.0	0.0008	5562.5	0.0008	5125.0	0.0008	5000.0
0.0009	6562.5	0.0009	6062.5	0.0009	5750.0	0.0009	5437.5
0.0010	7437.5	0.0010	6437.5	0.0010	6125.0	0.0010	6062.5
0.0011	7937.5	0.0011	6812.5	0.0011	6437.5	0.0011	6375.0
0.0012	8125.0	0.0012	7062.5	0.0012	6875.0	0.0012	6875.0
0.0013	8250.0	0.0013	7500.0	0.0013	7187.5	0.0013	7312.5
0.0014	8250.0	0.0014	7812.5	0.0014	7625.0	0.0014	7500.0
		0.0015	8187.5	0.0015	7750.0	0.0015	7875.0
		0.0016	8312.5	0.0016	8250.0	0.0016	8062.5
		0.0017	8750.0	0.0017	8312.5	0.0017	8250.0
		0.0018	9000.0	0.0018	8625.0	0.0018	8562.5
		0.0019	9062.5	0.0019	8875.0	0.0019	8687.0
		0.0020	9125.0	0.0020	8937.5	0.0020	9062.5
		0.0021	9125.0	0.0021	8937.5	0.0021	9062.5

SPECIMEN NUMBER 37		SPECIMEN NUMBER 38		SPECIMEN NUMBER 39		SPECIMEN NUMBER 40	
TIME IN SECONDS	FORCE IN POUNDS	TIME IN SECONDS	FORCE IN POUNDS	TIME IN SECONDS	FORCE IN POUNDS	TIME IN SECONDS	FORCE IN POUNDS
0.0001	937.5	0.0001	1250.0	0.0001	1187.5	0.0001	812.5
0.0002	2312.5	0.0002	2500.0	0.0002	2812.5	0.0002	1312.5
0.0003	3625.0	0.0003	3750.0	0.0003	3625.0	0.0003	2187.5
0.0004	4437.5	0.0004	4500.0	0.0004	4375.0	0.0004	3125.0
0.0005	5312.5	0.0005	5062.5	0.0005	5437.5	0.0005	3500.0
0.0006	5750.0	0.0006	5687.5	0.0006	5937.5	0.0006	4125.0
0.0007	6250.0	0.0007	6312.5	0.0007	6562.5	0.0007	4250.0
0.0008	7187.5	0.0008	6937.5	0.0008	7312.5	0.0008	4375.0
0.0009	7812.5	0.0009	8062.5	0.0009	7937.5	0.0009	4437.5
0.0010	8562.0	0.0010	8750.0	0.0010	8625.0	0.0010	4500.0
0.0011	9125.0	0.0011	9562.5	0.0011	9375.0	0.0011	4812.5
0.0012	9750.0	0.0012	10125.0	0.0012	10187.5	0.0012	5062.5
0.0013	10312.5	0.0013	10625.0	0.0013	10937.5	0.0013	5375.0
0.0014	10750.0	0.0014	11187.5	0.0014	11250.0	0.0014	5625.0
0.0015	11062.5	0.0015	11500.0	0.0015	11687.5	0.0015	5875.0
0.0016	11562.5	0.0016	11812.5	0.0016	12062.5	0.0016	6250.0
0.0017	11562.5	0.0017	11875.0	0.0017	12062.5	0.0017	6437.5
						0.0018	6562.5
						0.0019	6687.5
						0.0020	6875.0
						0.0021	6937.5
						0.0022	7000.0
						0.0023	7000.0
						0.0024	7000.0
						0.0025	7000.0

SPECIMEN NUMBER 41		SPECIMEN NUMBER 42		SPECIMEN NUMBER 43		SPECIMEN NUMBER 44	
TIME IN SECONDS	FORCE IN POUNDS	TIME IN SECONDS	FORCE IN POUNDS	TIME IN SECONDS	FORCE IN POUNDS	TIME IN SECONDS	FORCE IN POUNDS
0.0001	625.0	0.0001	625.0	0.0001	1500.0	0.0001	1875.0
0.0002	1187.5	0.0002	1250.0	0.0002	2875.0	0.0002	3750.0
0.0003	2000.0	0.0003	1937.0	0.0003	4937.5	0.0003	5000.0
0.0004	2875.0	0.0004	3062.5	0.0004	6000.0	0.0004	6000.0
0.0005	3625.0	0.0005	3687.5	0.0005	6625.0	0.0005	6437.5
0.0006	4062.5	0.0006	4062.5	0.0006	7062.5	0.0006	6875.0
0.0007	4250.0	0.0007	4375.0	0.0007	7375.0	0.0007	7375.0
0.0008	4312.5	0.0008	4500.0	0.0008	7750.0	0.0008	7812.0
0.0009	4437.5	0.0009	4562.5	0.0009	8062.5	0.0009	8125.0
0.0010	4562.5	0.0010	4625.0	0.0010	8437.5	0.0010	8500.0
0.0011	4750.0	0.0011	4875.0	0.0011	8687.5	0.0011	8625.0
0.0012	5000.0	0.0012	5125.0	0.0012	9000.0	0.0012	8812.5
0.0013	5375.0	0.0013	5562.5				
0.0014	5625.0	0.0014	5875.0				
0.0015	6000.0	0.0015	6250.0				
0.0016	6250.0	0.0016	6500.0				
0.0017	6562.5	0.0017	6625.0				
0.0018	6625.0	0.0018	6750.0				
0.0019	6687.5	0.0019	6937.5				
0.0020	6750.0	0.0020	7062.5				
0.0021	6812.5	0.0021	7187.5				
0.0022	6937.5	0.0022	7250.0				
0.0023	7062.5	0.0023	7250.0				
0.0024	7187.5	0.0024	7250.0				
0.0025	7187.5	0.0025	7250.0				

SPECIMEN NUMBER 45		SPECIMEN NUMBER 46		SPECIMEN NUMBER 47		SPECIMEN NUMBER 48	
TIME IN SECONDS	FORCE IN POUNDS	TIME IN SECONDS	FORCE IN POUNDS	TIME IN SECONDS	FORCE IN POUNDS	TIME IN SECONDS	FORCE IN POUNDS
0.0001	937.5	0.0001	625.0	0.0001	875.0	0.0001	625.0
0.0002	2687.5	0.0002	1250.0	0.0002	1625.0	0.0002	1250.0
0.0003	4500.0	0.0003	2125.0	0.0003	3125.5	0.0003	2500.0
0.0004	5750.0	0.0004	3625.0	0.0004	4250.0	0.0004	3687.5
0.0005	6500.0	0.0005	4500.0	0.0005	4875.0	0.0005	4562.5
0.0006	6875.0	0.0006	5000.0	0.0006	5625.0	0.0006	5375.0
0.0007	7187.5	0.0007	5687.5	0.0007	5875.0	0.0007	5562.5
0.0008	7625.0	0.0008	5812.5	0.0008	5937.5	0.0008	5750.0
0.0009	7812.5	0.0009	6000.0	0.0009	6062.5	0.0009	5812.5
0.0010	8250.0	0.0010	6125.0	0.0010	6125.0	0.0010	5937.5
0.0011	8375.0	0.0011	6187.5	0.0011	6187.5	0.0011	6062.5
0.0012	8750.0	0.0012	6250.0	0.0012	6312.5	0.0012	6187.5
0.0013	8750.0	0.0013	6312.5	0.0013	6500.0	0.0013	6312.5
		0.0014	6500.0	0.0014	6625.0	0.0014	6437.5
		0.0015	6625.0	0.0015	6750.0	0.0015	6562.5
		0.0016	6937.5	0.0016	6937.5	0.0016	6812.5
		0.0017	7062.5	0.0017	7312.5	0.0017	6937.5
		0.0018	7375.0	0.0018	7375.0	0.0018	7375.0
		0.0019	7437.5	0.0019	7437.5	0.0019	7375.0
		0.0020	7500.0	0.0020	7437.0	0.0020	7375.0
		0.0021	7500.0			0.0021	7375.0

SPECIMEN NUMBER 49		SPECIMEN NUMBER 50		SPECIMEN NUMBER 51		SPECIMEN NUMBER 52	
TIME IN SECONDS	FORCE IN POUNDS	TIME IN SECONDS	FORCE IN POUNDS	TIME IN SECONDS	FORCE IN POUNDS	TIME IN SECONDS	FORCE IN POUNDS
0.0001	875.0	0.0001	937.5	0.0001	812.5	0.0001	875.0
0.0002	1750.0	0.0002	1687.5	0.0002	1937.5	0.0002	1937.5
0.0003	2500.0	0.0003	2812.5	0.0003	3062.5	0.0003	2875.0
0.0004	4375.0	0.0004	4375.0	0.0004	3875.0	0.0004	3875.0
0.0005	5125.0	0.0005	5125.0	0.0005	4250.0	0.0005	4375.0
0.0006	5937.5	0.0006	5812.5	0.0006	4625.0	0.0006	4625.0
0.0007	6250.0	0.0007	6250.0	0.0007	4875.0	0.0007	5000.0
0.0008	6562.5	0.0008	6375.0	0.0008	5125.0	0.0008	5312.5
0.0009	6625.0	0.0009	6500.0	0.0009	5500.0	0.0009	5687.5
0.0010	6687.5	0.0010	6625.0	0.0010	5812.0	0.0010	6125.0
0.0011	6812.5	0.0011	6750.0	0.0011	6562.0	0.0011	6500.0
0.0012	6875.0	0.0012	6875.0	0.0012	7125.0	0.0012	7125.0
0.0013	7062.5	0.0013	7062.5	0.0013	7500.0	0.0013	7562.5
0.0014	7250.0	0.0014	7187.5	0.0014	7750.0	0.0014	7812.0
0.0015	7500.0	0.0015	7500.0	0.0015	8125.0	0.0015	8250.0
0.0016	7750.0	0.0016	7687.5	0.0016	8500.0	0.0016	8562.0
0.0017	7812.5	0.0017	7937.5	0.0017	8812.5	0.0017	8875.0
0.0018	8062.5	0.0018	8125.0	0.0018	9250.0	0.0018	9187.0
0.0019	8125.0	0.0019	8125.0	0.0019	9375.0	0.0019	9500.0
0.0020	8125.0	0.0020	8125.0	0.0020	9375.0	0.0020	9562.0
				0.0021	9375.0	0.0021	9562.0

SPECIMEN NUMBER 53

TIME IN SECONDS	FORCE IN POUNDS
0.0001	750.0
0.0002	1625.0
0.0003	2625.0
0.0004	3875.0
0.0005	4437.5
0.0006	4687.5
0.0007	5125.0
0.0008	5312.5
0.0009	5750.0
0.0010	6250.0
0.0011	6812.5
0.0012	7187.5
0.0013	7562.5
0.0014	8000.0
0.0015	8250.0
0.0016	8437.5
0.0017	8875.0
0.0018	9062.5
0.0019	9375.0
0.0020	9375.0
0.0021	9375.0

SPECIMEN NUMBER 54

TIME IN SECONDS	FORCE IN POUNDS
0.0001	375.0
0.0002	687.5
0.0003	1500.0
0.0004	2500.0
0.0005	2875.0
0.0006	3250.0
0.0007	3312.5
0.0008	3375.0
0.0009	3500.0
0.0010	3625.0
0.0011	3812.5
0.0012	3937.5
0.0013	4375.0
0.0014	4500.0
0.0015	4687.5
0.0016	4875.0
0.0017	5000.0
0.0018	5062.5
0.0019	5125.0
0.0020	5187.5
0.0021	5250.0
0.0022	5312.5
0.0023	5375.0
0.0024	5375.0
0.0025	5375.0

SPECIMEN NUMBER 55

TIME IN SECONDS	FORCE IN POUNDS
0.0001	750.0
0.0002	1875.0
0.0003	2687.5
0.0004	3250.0
0.0005	3562.5
0.0006	3687.5
0.0007	3937.5
0.0008	4250.0
0.0009	4437.5
0.0010	4750.0
0.0011	5187.5
0.0012	5500.0
0.0013	5625.0
0.0014	5812.5
0.0015	6000.0
0.0016	6187.5
0.0017	6375.0
0.0018	6500.0
0.0019	6562.0
0.0020	6625.0
0.0021	6625.0
0.0022	6625.0

SPECIMEN NUMBER 56

TIME IN SECONDS	FORCE IN POUNDS
0.0001	937.5
0.0002	1500.0
0.0003	2875.0
0.0004	3625.0
0.0005	3750.0
0.0006	3875.0
0.0007	4125.0
0.0008	4312.5
0.0009	4562.5
0.0010	5000.0
0.0011	5375.0
0.0012	5500.0
0.0013	5687.5
0.0014	5875.0
0.0015	6125.0
0.0016	6250.0
0.0017	6437.5
0.0018	6625.0
0.0019	6687.0
0.0020	6750.0
0.0021	6750.0
0.0022	6750.0

SPECIMEN NUMBER 57		SPECIMEN NUMBER 58		SPECIMEN NUMBER 59		SPECIMEN NUMBER 60	
TIME IN SECONDS	FORCE IN POUNDS	TIME IN SECONDS	FORCE IN POUNDS	TIME IN SECONDS	FORCE IN POUNDS	TIME IN SECONDS	FORCE IN POUNDS
0.0001	707.2	0.0001	832.0	0.0001	707.2	0.0001	748.8
0.0002	1747.0	0.0002	2080.0	0.0002	1705.6	0.0002	1497.6
0.0003	2662.4	0.0003	3369.6	0.0003	2704.0	0.0003	2662.4
0.0004	3411.2	0.0004	4284.8	0.0004	3868.8	0.0004	3161.6
0.0005	3660.8	0.0005	5033.6	0.0005	4492.8	0.0005	3411.2
0.0006	3827.2	0.0006	5366.4	0.0006	5116.8	0.0006	3577.6
0.0007	3952.0	0.0007	5408.0	0.0007	5324.8	0.0007	3744.0
0.0008	4243.2	0.0008	5449.6	0.0008	5408.0	0.0008	3827.2
0.0009	4492.8	0.0009	5491.2	0.0009	5449.6	0.0009	3910.4
0.0010	4784.0	0.0010	5532.8	0.0010	5491.2	0.0010	3993.6
0.0011	5200.0	0.0011	5616.0	0.0011	5532.8	0.0011	4243.2
0.0012	5408.0	0.0012	5657.6	0.0012	5574.4	0.0012	4409.6
0.0013	5574.4	0.0013	5782.4	0.0013	5740.8	0.0013	4659.2
0.0014	5907.2	0.0014	6032.0	0.0014	5948.8	0.0014	4825.6
0.0015	6037.0	0.0015	6198.4	0.0015	6032.0	0.0015	4950.4
0.0016	6281.6	0.0016	6323.2	0.0016	6323.2	0.0016	5075.2
0.0017	6406.4	0.0017	6406.4	0.0017	6364.8	0.0017	5116.8
0.0018	6489.6	0.0018	6572.8	0.0018	6448.0	0.0018	5200.0
0.0019	6531.2	0.0019	6572.8	0.0019	6489.6	0.0019	5241.0
0.0020	6614.4	0.0020	6572.8	0.0020	6489.6	0.0020	5283.2
0.0021	6614.4					0.0021	5324.8
0.0022	6614.4					0.0022	5324.8
						0.0023	5324.8
						0.0024	5324.8

SPECIMEN NUMBER 61

TIME IN SECONDS	FORCE IN POUNDS
0.0001	332.8
0.0002	873.6
0.0003	1580.8
0.0004	2412.8
0.0005	2953.6
0.0006	3369.6
0.0007	3577.6
0.0008	3660.8
0.0009	3785.6
0.0010	3827.2
0.0011	3993.6
0.0012	4160.0
0.0013	4451.2
0.0014	4659.2
0.0015	4867.2
0.0016	5033.6
0.0017	5158.4
0.0018	5241.6
0.0019	5324.8
0.0020	5366.0
0.0021	5408.0
0.0022	5408.0
0.0023	5449.6
0.0024	5491.0
0.0025	5532.8

SPECIMEN NUMBER 62

TIME IN SECONDS	FORCE IN POUNDS
0.0001	1062.5
0.0002	2312.5
0.0003	3750.0
0.0004	5187.5
0.0005	5687.5
0.0006	6250.0
0.0007	6500.0
0.0008	6875.0
0.0009	7187.5
0.0010	7500.0
0.0011	7875.0
0.0012	8125.0
0.0013	8375.0
0.0014	8562.5
0.0015	8625.0
0.0016	8625.0

SPECIMEN NUMBER 63

TIME IN SECONDS	FORCE IN POUNDS
0.0001	937.5
0.0002	2687.5
0.0003	4312.5
0.0004	5250.0
0.0005	5812.0
0.0006	6250.0
0.0007	6437.5
0.0008	6875.0
0.0009	7312.5
0.0010	7625.0
0.0011	8062.5
0.0012	8250.0
0.0013	8437.5
0.0014	8750.0
0.0015	8750.0
0.0016	8750.0

SPECIMEN NUMBER 64

TIME IN SECONDS	FORCE IN POUNDS
0.0001	1331.2
0.0002	2787.2
0.0003	4160.0
0.0004	4409.6
0.0005	4742.4
0.0006	5033.6
0.0007	5158.4
0.0008	5740.8
0.0009	5865.6
0.0010	6073.6
0.0011	6240.0
0.0012	6323.2
0.0013	6364.8
0.0014	6364.8
0.0015	6364.8

SPECIMEN NUMBER 65		SPECIMEN NUMBER 66		SPECIMEN NUMBER 67		SPECIMEN NUMBER 68	
TIME IN SECONDS	FORCE IN POUNDS	TIME IN SECONDS	FORCE IN POUNDS	TIME IN SECONDS	FORCE IN POUNDS	TIME IN SECONDS	FORCE IN POUNDS
0.0001	956.8	0.0001	998.4	0.0001	540.8	0.0001	540.8
0.0002	2620.8	0.0002	1830.4	0.0002	1372.8	0.0002	1580.8
0.0003	3868.8	0.0003	2620.8	0.0003	2204.8	0.0003	2371.2
0.0004	4492.8	0.0004	2828.8	0.0004	2745.6	0.0004	2787.2
0.0005	4784.0	0.0005	3036.8	0.0005	2995.2	0.0005	2995.2
0.0006	5075.2	0.0006	3161.6	0.0006	3078.4	0.0006	3036.8
0.0007	5200.0	0.0007	3244.8	0.0007	3203.2	0.0007	3203.2
0.0008	5532.8	0.0008	3411.2	0.0008	3411.2	0.0008	3328.0
0.0009	5782.4	0.0009	3619.2	0.0009	3577.6	0.0009	3619.2
0.0010	5948.8	0.0010	3827.2	0.0010	3785.6	0.0010	3785.6
0.0011	6156.8	0.0011	4035.2	0.0011	3993.6	0.0011	3952.0
0.0012	6240.0	0.0012	4118.4	0.0012	4201.6	0.0012	4160.0
0.0013	6281.6	0.0013	4243.2	0.0013	4284.8	0.0013	4284.8
0.0014	6323.0	0.0014	4326.4	0.0014	4326.4	0.0014	4326.4
0.0015	6323.0	0.0015	4409.6	0.0015	4451.2	0.0015	4451.2
		0.0016	4451.2	0.0016	4534.4	0.0016	4534.4
		0.0017	4492.8	0.0017	4617.6	0.0017	4576.0
		0.0018	4534.4	0.0018	4700.8	0.0018	4617.6
		0.0019	4576.0	0.0019	4742.4	0.0019	4617.6
		0.0020	4576.0	0.0020	4742.4	0.0020	4617.6

I	D	C	B	H	W	VO	XA	AXEDOT	PED	PXD
1	0.993	0.952	0.519	364.0	6.81	43.1	0.433	271.7	91.5	-13.9
2	0.992	0.951	0.502	364.0	6.81	43.1	0.449	272.0	91.4	-20.3
3	0.992	0.949	0.506	364.0	6.81	43.1	0.443	272.6	88.7	-24.9
4	0.992	0.949	0.512	364.0	6.81	43.1	0.437	272.6	91.2	-23.1
5	0.990	0.959	0.506	364.0	6.81	43.1	0.453	269.7	89.7	-21.2
6	0.991	0.957	0.560	288.0	6.81	38.3	0.397	240.4	89.2	-22.5
7	0.991	0.954	0.562	288.0	6.81	38.3	0.392	241.1	93.8	-18.6
8	0.994	0.945	0.551	288.0	6.81	38.3	0.394	243.5	94.8	-16.4
9	0.991	0.941	0.613	207.0	6.81	32.5	0.328	207.3	93.8	-28.1
10	0.991	0.949	0.623	207.0	6.81	32.5	0.326	205.5	93.2	-20.4
11	0.991	0.951	0.635	207.0	6.81	32.5	0.316	205.1	90.9	-26.6
12	0.993	0.940	0.711	120.0	6.81	24.8	0.229	158.0	85.8	-39.0
13	0.991	0.945	0.718	120.0	6.81	24.8	0.227	157.2	81.5	-33.7
14	0.992	0.955	0.724	120.0	6.81	24.7	0.231	155.5	78.3	-33.3
15	0.993	0.953	0.645	120.0	10.44	24.9	0.308	157.0	86.3	-27.0
16	0.993	0.960	0.658	120.0	10.44	24.9	0.302	155.8	88.5	-34.5
17	0.991	0.959	0.654	120.0	10.44	24.9	0.305	156.0	85.4	-28.5
18	0.993	0.961	0.652	120.0	10.44	24.9	0.309	155.7	86.6	-25.4
19	0.992	0.950	0.526	207.0	10.44	32.8	0.424	206.9	92.4	-23.8
20	0.993	0.957	0.529	207.0	10.44	32.7	0.428	205.3	93.6	-29.0
21	0.993	0.955	0.536	207.0	10.44	32.8	0.419	205.8	94.4	-29.8
22	0.991	0.957	0.450	288.0	10.44	38.6	0.507	242.2	92.3	-17.0
23	0.992	0.955	0.443	288.0	10.44	38.6	0.512	242.7	92.3	-15.3
24	0.991	0.969	0.462	288.0	10.44	38.6	0.507	239.2	92.2	-23.8
25	0.992	0.963	0.459	360.0	8.63	43.1	0.504	268.3	90.9	-15.7
26	0.991	0.951	0.444	360.0	8.63	43.1	0.507	271.7	87.4	-19.5
27	0.993	0.958	0.439	360.0	8.63	43.1	0.519	269.7	91.9	-20.2
28	0.993	0.955	0.401	432.0	8.63	47.2	0.554	296.4	89.6	-17.4
29	0.992	0.956	0.409	432.0	8.63	47.2	0.547	296.1	90.3	-19.3
30	0.993	0.956	0.401	432.0	8.63	47.2	0.555	296.0	89.3	-19.1
31	0.994	0.958	0.464	434.0	6.81	47.1	0.494	294.7	89.9	-22.7
32	0.993	0.944	0.461	434.0	6.81	47.1	0.483	299.2	91.3	-23.8
33	0.993	0.950	0.451	434.0	6.81	47.1	0.499	297.3	92.1	-18.8
34	0.991	1.461	0.757	359.5	10.44	42.8	0.704	175.9	99.8	4.6

I	D	C	B	H	W	VO	XA	AXEDOT	PED	PXD
35	0.992	1.451	0.752	359.5	10.44	42.8	0.699	177.2	99.3	0.3
36	0.993	1.465	0.762	359.5	10.44	42.8	0.703	175.4	99.0	-0.8
37	0.992	0.951	0.386	360.0	10.44	43.2	0.565	272.5	98.3	-6.6
38	0.991	0.949	0.389	360.0	10.44	43.2	0.560	273.1	98.8	-6.4
39	0.993	0.955	0.393	360.0	10.44	43.2	0.562	271.4	99.1	-5.1
40	0.992	1.967	1.163	359.0	10.44	42.5	0.804	129.6	99.4	-1.0
41	0.992	1.981	1.167	359.0	10.44	42.5	0.814	128.7	99.3	-0.5
42	0.994	1.953	1.152	359.0	10.44	42.5	0.801	130.5	99.7	-0.6
43	1.243	1.244	0.843	359.8	6.81	41.9	0.396	202.1	98.4	-0.8
44	1.241	1.244	0.859	359.8	6.81	41.9	0.385	202.1	98.7	-1.8
45	1.240	1.220	0.840	359.8	6.81	41.9	0.380	206.3	99.6	-9.8
46	1.241	2.460	1.812	358.5	10.44	41.3	0.648	100.8	98.9	-4.0
47	1.241	2.460	1.815	358.5	10.44	41.3	0.645	100.8	98.4	0.4
48	1.239	2.472	1.797	358.5	10.44	41.3	0.675	100.3	98.8	0.4
49	1.237	2.457	1.711	430.5	10.44	45.3	0.746	110.6	97.9	4.0
50	1.239	2.457	1.730	430.5	10.44	45.3	0.727	110.6	97.9	1.4
51	0.993	1.454	0.683	431.5	10.44	46.9	0.771	193.7	97.8	-4.4
52	0.993	1.459	0.692	431.5	10.44	46.9	0.767	193.0	98.1	-4.3
53	0.993	1.558	0.682	431.5	10.44	46.9	0.876	180.5	98.1	8.8
54	0.993	1.973	1.333	240.0	10.44	34.7	0.640	105.6	98.4	-7.1
55	0.992	1.459	0.890	240.5	10.44	35.0	0.569	144.1	99.5	-2.8
56	0.992	1.457	0.892	240.5	10.44	35.0	0.565	144.3	99.8	-1.8
57	0.991	1.455	0.888	240.5	10.44	35.0	0.567	144.5	99.5	-2.9
58	1.240	2.476	1.954	239.8	10.44	33.8	0.522	81.9	****	8.4
59	1.241	2.456	1.933	239.8	10.44	33.8	0.523	82.6	99.7	5.2
60	0.992	1.966	1.320	240.0	10.44	34.7	0.646	106.0	98.9	2.5
61	0.992	1.971	1.319	240.0	10.44	34.7	0.652	105.7	99.1	-2.7
62	1.242	1.237	0.849	240.8	10.44	34.8	0.388	168.9	98.9	-11.9
63	1.243	1.214	0.825	240.8	10.44	34.8	0.389	172.1	99.2	-10.2
64	1.241	1.236	0.984	120.0	10.44	24.6	0.252	119.3	99.8	-6.6
65	1.241	1.223	0.976	120.0	10.44	24.6	0.247	120.6	99.6	-10.9
66	0.992	1.456	1.083	120.0	10.44	24.8	0.373	102.0	98.8	-0.1
67	0.993	1.437	1.069	120.0	10.44	24.8	0.368	103.4	98.5	-4.3
68	0.992	1.457	1.092	120.0	10.44	24.8	0.365	101.9	98.5	-4.6

APPENDIX B

MATHEMATICAL JUSTIFICATIONS AND DERIVATION OF EQUATIONS

Demonstration of the validity of Equations 5.4 and 5.5 and the derivation of Fortran equations in Statements 1920, 2570, and 2700 of the computer program are presented in this Appendix.

Validity of Equations 5.4 and 5.5

In the derivation of Equations 5.4 and 5.5, it was assumed that the difference between the time, Δt_a, required for the velocity of the free-falling weight and the velocity of the top of the specimen to become equal and the time, Δt_s, required for the stress wave to propagate the length of the specimen is negligible. Hence, the external force that might be applied to the bottom of the specimen is negligible. The validity of this assumption is demonstrated as follows.

For this time interval, it was assumed that the stress in the specimen has not exceeded the elastic limit and that the material obeys Hooke's Law. A linear velocity-time relationship was also assumed. By the principles of impulse and momentum,

$$\int_{o}^{\Delta t_a} F' \, dt = M_w(V_o' - V_o) \tag{B.1}$$

where

F' = impulse force at any time,

t = time,

M_w = mass of falling weight,

V'_o = velocity of falling weight just prior to contacting the specimen, and

V_o = velocity at the time the velocity of the weight and the velocity of the top of the specimen are equal.

Since the material of the specimen obeys Hooke's Law

$$F = \frac{\sigma}{2}A = \frac{E\epsilon A}{2} \tag{B.2}$$

where

F = average force applied to the specimen,

σ = maximum stress in the specimen during the time interval,

A = cross-sectional area of the specimen,

E = modulus of elasticity of the specimen, and

ϵ = maximum strain in the specimen during the time interval.

Therefore, Equation B.1 becomes

$$\int_o^{\Delta t_a} F\ dt = \frac{E\epsilon A(\Delta t_a)}{2}$$

$$= M_w(V'_o - V_o)\ . \tag{B.3}$$

Since the deflection of the specimen, assuming a linear velocity-time relationship,

$$X = \int_o^{\Delta t_a} V\ dt = \frac{V_o}{2}(\Delta t_a) \tag{B.4}$$

where

V = velocity,

V_o = velocity at the time the velocity of the weight and the velocity of the top of the specimen are equal, and

Δt_a = time required for the velocity of the free-falling weight and the velocity of the top of the specimen to become equal;

by the definition of strain

$$\epsilon = \frac{X}{L} = \frac{V_o}{2L}(\Delta t_a) \tag{B.5}$$

where

X = deflection of the specimen and

L = the initial length of the specimen.

Substituting for ϵ, Equation B.3 becomes

$$\frac{EV_oA(\Delta t_a)^2}{4L} = M_w(V_o' - V_o) \ . \tag{B.6}$$

Solving Equation B.6 for Δt_a,

$$\Delta t_a = \left[\frac{4LM_w}{EA}\left(\frac{V_o'}{V_o} - 1\right)\right]^{1/2} \ . \tag{B.7}$$

Substituting $(2gh)^{1/2}$ for V_o'

where

g = gravitational acceleration and

h = drop height of weight in inches,

and, from Equation 5.5 on page 35,

$$\frac{(2gh)^{1/2}}{1 + \frac{\pi D^2 L\rho}{8W_w}} \quad \text{for } V_o$$

where

D = initial diameter of specimen,

L = initial length of specimen,

ρ = density of specimen, and

W_w = weight of free-falling weight;

Equation B.7 becomes

$$\Delta t_a = \left[\frac{4LM_w}{EA}\left(\frac{(2gh)^{1/2}}{\dfrac{(2gh)^{1/2}}{1 + \dfrac{\pi D^2 L\rho}{8W_w}}} - 1\right)\right]^{1/2} .$$

Simplifying,

$$\Delta t_a = \left[\frac{4LM_w}{EA}\left(\frac{\pi D^2 L\rho}{8W_w}\right)\right]^{1/2}$$

$$= \left(\frac{2L^2\rho}{Eg}\right)^{1/2} \tag{B.8}$$

The well-known equation for the velocity of a stress wave in an elastic material

$$V_s = \left(\frac{Eg}{\rho}\right)^{1/2} = \frac{L}{\Delta t_s} , \tag{B.9}$$

where

V_s = the velocity of the stress wave and

Δt_s = the time required for the stress wave to propagate the length of the specimen,

may be solved for Δt_s to yield

$$\Delta t_s = \left(\frac{L^2\rho}{Eg}\right)^{1/2} \tag{B.10}$$

Using Equations B.8 and B.10, the ratio

$$\frac{\Delta t_a}{\Delta t_s} = \frac{\left(\dfrac{2L^2\rho}{Eg}\right)^{1/2}}{\left(\dfrac{L^2\rho}{Eg}\right)^{1/2}} = (2)^{1/2}$$

$$= 1.41 . \tag{B.11}$$

From Equation B.10

$$\Delta t_s = L\left(\frac{\rho}{Eg}\right)^{1/2}$$

where values of

$L = 2.5$ inches (maximum length of specimen tested),

$\rho = 0.41$ pounds per cubic inch,

$E = 2 \times 10^6$ pounds per square inch, and

$g = 384$ inches per second per second

were used; the maximum value of

$$\Delta t_s = 0.0000577 \text{ seconds.}$$

From the ratio expressed in Equation B.11, the maximum value of

$$\Delta t_a = 0.0000814 \text{ seconds.}$$

The difference between Δt_a and Δt_s is 0.0000237 seconds. From the assumption of a linear velocity-time and stress-strain relationship, it follows that the force-time relationship is also linear. Thus, the force at this time may be computed. The maximum force recorded for any specimen tested at the time of 0.0001 seconds was 1,614 pounds. By similar triangles, the force applied to the bottom of the specimen at this time would be approximately 380 pounds, which is in fact negligible.

Derivation of Fortran Statements 1920, 2570, and 2700

The percentage of kinetic energy accounted for is computed by the Fortran equation in Statement 1920 of the computer program. This percentage of the available kinetic energy accounted for is based on the difference between the kinetic energy possessed by the system at time equal zero (when the velocity is equal to the initial velocity) and the

kinetic energy indicated by the computed velocity at the last data point (point of maximum force). At time equal zero, the kinetic energy possessed by the system

$$KE_o = \frac{1}{2} M[VO_{(I)}]^2 \tag{B.12}$$

where

KE_o = kinetic energy at time equal zero,

M = mass of the system, and

$VO_{(I)}$ = velocity of the system.

Without exception, the computer calculations indicated that after the maximum force had been recorded and the velocity had in fact become zero, the weight had a downward velocity and therefore possessed indicated kinetic energy of

$$KE_F = \frac{1}{2} M[V_{(I,J')}]^2 \tag{B.13}$$

where

KE_F = indicated kinetic energy,

M = mass of the system, and

$V_{(I,J')}$ = indicated velocity when the actual velocity is zero.

The quantity of kinetic energy that the data acquisition and transformation system accounts for is the difference between the quantities KE_o and KE_F. Therefore, the equation that is used to compute the percentage of kinetic energy accounted for

$$PED_{(I)} = \frac{[VO_{(I)}]^2 - [V_{(I,J')}]^2}{[VO_{(I)}]^2}(100) \tag{B.14}$$

is an arbitrary measure of the accuracy of the data acquisition and

translation system. After substitution of constants, Equation B.14 is equivalent to the Fortran equation in Statement 1920 of the computer program.

A compressive specimen, located on top of a rigid surface, that is being deformed by a moving mass will undergo a displacement of Vt where V = velocity and t = time. Assuming a linear velocity profile, the displacement, u, of any point a distance X above the rigid surface will be

$$u = \frac{VtX}{L} \tag{B.15}$$

where L = the length of the specimen. It follows that the strain, ϵ, will be

$$\epsilon = \frac{\partial u}{\partial X} = \frac{Vt}{L} . \tag{B.16}$$

In turn, the strain rate will be

$$\frac{\partial \epsilon}{\partial t} = \frac{V}{L} . \tag{B.17}$$

Equation B.17 is equivalent to the Fortran equation given in Statement 2570 of the computer program. This equation is as follows.

$$XEDOT_{(I)} = \frac{V_{(I,J)}}{C_{(I)} - X_{(I,J)}} \tag{B.18}$$

where

$XEDOT_{(I)}$ = strain rate,

$C_{(I)}$ = initial length of specimen, and

$X_{(I,J)}$ = deformation of specimen.

The Fortran equation in Statement 2700 of the computer program computes the average strain rate. The average strain rate may be defined as the velocity or rate at which two points on a body approach or

diverge from each other averaged over the entire deformation period divided by the initial distance between these points. The ends of each specimen tested were selected as the two points, and the equation for average strain rate is

$$AXEDOT_{(I)} = \frac{\frac{VO_{(I)}}{2}(12)}{C_{(I)}} \tag{B.19}$$

where

$AXEDOT_{(I)}$ = average strain rate,

$VO_{(I)}$ = initial velocity, and

$C_{(I)}$ = initial length of specimen.

Equation B.19 is equivalent to the Fortran equation in Statement 2700 of the computer program.

VITA

John Harper Evans was born in Kingston, Tennessee, on July 19, 1934. He attended elementary and high schools in Rockwood, Tennessee, and was graduated from Rockwood High School in June, 1952. The following September he entered Tennessee Polytechnic Institute, and in June, 1956, he received a Bachelor of Science degree in Mechanical Engineering. Following graduation, he was employed at the Oak Ridge Gaseous Diffusion Plant. In July of 1961, he transferred to Oak Ridge National Laboratory, which is operated by Union Carbide Corporation for the United States Atomic Energy Commission, where he is employed at present.

He entered the Graduate School at The University of Tennessee in September, 1965, and received the Master of Science degree in Mechanical Engineering in June, 1970. He is a Licensed Professional Engineer, a member of the National Society of Professional Engineers, and a member of the Society for Experimental Stress Analysis.

Internal Distribution

1. M. Bender
2. C. E. Bettis
3. F. R. Bruce
4. D. D. Cannon
5. G. B. Child
6. F. L. Culler, Jr.
7. F. C. Davis
8. R. L. Donahue
9. H. G. Duggan
10-14. J. H. Evans
15. W. F. Ferguson
16. F. C. Fitzpatrick
17. F. J. Furman, Jr.
18. W. R. Gall
19. J. H. Gillette
20. K. W. Haff
21. A. R. Irvine
22. E. M. King
23. B. B. Klima
24. R. J. Lauer
25. A. J. Mallett (K-25)
26. J. R. McGuffey
27. J. D. McLendon (Y-12)
28. H. A. Nelms
29. J. D. Rollins
30. A. F. Rupp
31. R. A. Schmidt
32. R. D. Seagren
33-37. L. B. Shappert
38. W. C. Stoddart
39. J. Thomas
40. W. E. Unger
41. H. K. Walker
42. D. C. Watkin
43. W. R. Winsbro
44-45. Central Research Library
46. Document Reference Section
47. GE Division Library
48-60. Laboratory Records Department
61. Laboratory Records, ORNL R.C.
62. ORNL Patent Office

External Distribution

63. F. E. Adcock, The Dow Chemical Company, Rocky Flats Division, Post Office Box 888, Golden Colorado 80401
64. A. E. Aikens, Jr., Capintec, Inc., 527 Madison Avenue, Suite 920, New York, New York 10022
65. W. L. Albrecht, Tennessee Valley Authority, New Sprankle Building, Knoxville, Tennessee 37902

66. A. Anselmo, Idaho Nuclear Corporation, Post Office Box 1845, Idaho Falls, Idaho 83401

67. R. F. Barker, USAEC, Division of Radiation Protection, Washington, D. C. 20545

68. R. J. Bass, E. I. du Pont de Nemours & Company, Savannah River Plant, Aiken, South Carolina 29801

69. W. G. Belter, USAEC, Division of Reactor Development and Technology, Washington, D. C. 20545

70. S. Bernstein, Union Carbide Corporation, Post Office Box 1410, Paducah, Kentucky 42001

71. R. L. Bragg, Nuclear Materials and Equipment Corporation, Apollo, Pennsylvania 15613

72. W. A. Brobst, U. S. Department of Transportation, 6th and D Street SW, Washington, D. C. 20590

73. C. L. Brown, Pacific Northwest Laboratory, Richland, Washington 99352

74. J. F. Brown, National Lead Company, Foot of West Street, Wilmington, Delaware 19898

75. J. S. Brown, Tennessee Technological University, Cookeville, Tennessee 38501

76. C. W. Buckland, Los Alamos Scientific Laboratory, Post Office Box 1663, Los Alamos, New Mexico 87544

77. H. G. Clarke, Jr., The Franklin Institute Laboratories, Twentieth and Parkway, Philadelphia, Pennsylvania 19103

78. J. E. Conway, E. I. du Pont de Nemours & Company, Savannah River Plant, Aiken, South Carolina 29801

79. C. M. Copenhauer, USAEC, Oak Ridge Operations Office, Post Office Box E, Oak Ridge, Tennessee 37830

80. J. J. Cullen, National Lead Company, 1050 State Street, Perth Amboy, New Jersey 08862

81. T. E. Dabrowski, Douglas United Nuclear, Inc., Post Office Box 490, Richland, Washington 99352

82. A. W. DeMerschman, Pacific Northwest Laboratory, Post Office Box 999, Richland, Washington 99352

83. B. D. Devine, Argonne National Laboratory, 9700 South Cass Avenue, Argonne, Illinois 60439

84. D. L. Dunaway, National Lead Company of Ohio, Post Office Box 39158, Cincinnati, Ohio 45239

85. D. A. Edling, Mound Laboratory, Monsanto Research Corporation, Miamisburg, Ohio 45342

86. A. J. Edmondson, Department of Mechanical Engineering, The University of Tennessee, Knoxville, Tennessee 37916

87. C. S. Ehrman, Allied Chemical Corporation, Post Office Box 35, Florham Park, New Jersey 07932

88. T. R. Emswiler, Battelle Memorial Institute, 505 King Avenue, Columbus, Ohio 43201

89. J. T. Foley, Sandia Laboratories, Post Office Box 5800, Albuquerque, New Mexico 87115

90. W. P. Gammill, USAEC, Division of Reactor Development and Technology, Washington, D. C. 20545

91. C. Glidewell, Tennessee Valley Authority, 200 Arnstein Building, Knoxville, Tennessee 37902

92. A. W. Grella, U. S. Department of Transportation, 6th and D Street SW, Washington, D. C. 20590

93. T. Gutman, Westinghouse Electric Corporation, Post Office Box 217, Cheswick, Pennsylvania 15024

94. R. W. Holland, Department of Mechanical Engineering, The University of Tennessee, Knoxville, Tennessee 37916

95. D. A. Hoover, Atlantic Richfield Hanford Company, Richland, Washington 99352

96. L. H. Horn, Underwriters' Laboratories, 207 E. Ohio Street, Chicago, Illinois 60611

97. W. R. Householder, HGS Technical Associates, Inc., Post Office Box 1156, Johnson City, Tennessee 37601

98. P. C. Huang, Bureau of Naval Ordnance Laboratory, Silver Spring, Maryland 20907

99. R. I. Jetter, Atomics International, Post Office Box 309, Canoga Park, California 91304

100. J. W. Jones, Bettis Atomic Power Laboratory, Post Office Box 79, West Mifflin, Pennsylvania 15122

101. B. A. Karrasch, The Babcock & Wilcox Company, Post Office Box 1260, Lynchburg, Virginia 24505

102. R. E. Kropp, United Nuclear Corporation, Post Office Box 1883, New Haven, Connecticut 06508

103. W. Legler, Allied Chemical, In care of Bectel Corporation, 50 Beale Street, San Francisco, California 94105

104. J. W. Langhaar, E. I. du Pont de Nemours & Company, Wilmington, Delaware, 19898

105. B. G. Lindberg, USAEC, Division of Materials Licensing, Washington, D. C. 20545

106. R. E. Lipenski, USAEC, Division of Materials Licensing, Washington, D. C. 20545

107. E. C. Lusk, Battelle Memorial Institute, 505 King Avenue, Columbus, Ohio 43201

108. R. J. Lusky, National Lead Company, 1130 Central Avenue, Albany, New York 12205

109. W. C. McCluggage, USAEC, Division of Operational Safety, Washington, D. C. 20545

110-111. J. S. Milau, Brookhaven National Laboratory, Upton, L. I., New York 11973

112. W. A. Nelson, USAEC, Division of Reactor Development and Technology, Washington, D. C. 20545

113. H. E. Noyes, Los Alamos Scientific Laboratory, Post Office Box 1663, Los Alamos, New Mexico 87544

114. R. H. Odegaarden, USAEC, Division of Materials Licensing, Washington, D. C. 20545

115. R. W. Peterson, Allied Chemical Corporation, Post Office Box 35, Florham Park, New Jersey 07932

116. H. Pih, Department of Engineering Mechanics, The University of Tennessee, Knoxville, Tennessee 37916

117. W. A. Pryor, USAEC, Oak Ridge Operations, Post Office Box E, Oak Ridge, Tennessee 37830

118. S. L. Reese, Nuclear Safety Associates, Suite 200, 7735 Old Georgetown Road, Bethesda, Maryland 20014

119. R. F. Rogers, E. I. du Pont de Nemours & Company, Savannah River Plant, Aiken, South Carolina 29801

120. W. F. Romine, The Dow Chemical Company, Rocky Flats, Golden, Colorado 80401

121. H. P. Shaw, Atlantic Richfield Hanford Company, Post Office Box 250, Richland, Washington 99352

122. L. R. Shobe, Department of Engineering Mechanics, The University of Tennessee, Knoxville, Tennessee 37916

123. J. A. Sisler, USAEC, Traffic Management Branch, Washington, D. C. 20545

124. C. W. Smith, General Electric Company, 283 Brokaw Road, Santa Clara, California 95050

125. D. R. Smith, Los Alamos Scientific Laboratory, Post Office Box 1663, Los Alamos, New Mexico 87544

126. F. H. Speckhart, Department of Mechanical Engineering, The University of Tennessee, Knoxville, Tennessee 37916

127. D. R. Swindle, USAEC, Division of Construction, Washington, D. C. 20545

128. R. J. Thompson, Stearns-Roger Coperation, Post Office Box 5888, Denver Colorado 80217

129. H. E. Walchli, Westinghouse Electric Corporation, Post Office Box 355, Pittsburgh, Pennsylvania 15230

130. R. B. Waite, Stearns-Roger Corporation, Post Office Box 5888, Denver, Colorado 80217

131-145. Division of Technical Information Extension, USAEC

146. Laboratory and University Division, USAEC, ORO